JOURNAL OF GEOPHYSICAL RESEARCH, VOL. 103, NO. D22, PAGES 28,721-28,742, NOVEMBER 27, 1998

Stable isotope composition of precipitation over southeast Asia

Luis Araguás-Araguás[1] and Klaus Froehlich

Isotope Hydrology Section, International Atomic Energy Agency, Vienna, Austria

Kazimierz Rozanski

Faculty of Physics and Nuclear Techniques, University of Mining and Metallurgy, Krakow, Poland

Abstract. Spatial and temporal variability of the stable isotope composition of precipitation in the southeast Asia and western Pacific region is discussed, with emphasis on the China territory, based on the database of the International Atomic Energy Agency/World Meteorological Organization Global Network "Isotopes in Precipitation" and the available information on the regional climatology and atmospheric circulation patterns. The meteorological and pluviometric regime of southeast Asia is controlled by five different air masses: (1) polar air mass originating in the Arctic, (2) continental air mass originating over central Asia, (3) tropical-maritime air mass originating in the northern Pacific, (4) equatorial-maritime air mass originating in the western equatorial Pacific, and (5) equatorial-maritime air mass originating in the Indian Ocean. The relative importance of different air masses in the course of a given year is modulated by the monsoon activity and the seasonal displacement of the Intertropical Convergence Zone (ITCZ). Gradual rain-out of moist, oceanic air masses moving inland, associated with monsoon circulation, constitutes a powerful mechanism capable of producing large isotopic depletions in rainfall, often completely overshadowing the dependence of $\delta^{18}O$ and $\delta^{2}H$ on temperature. For instance, precipitation at Lhasa station (Tibetan Plateau) during rainy period (June-September) is depleted in ^{18}O by more than 6 $^{o}/_{oo}$ with respect to winter rainfall, despite of 10°C higher surface air temperature in summer. This characteristic isotopic imprint of monsoon activity is seen over large areas of the region. The oceanic air masses forming the two monsoon systems, Pacific and Indian monsoon, differ in their isotope signatures, as demonstrated by the average $\delta^{18}O$ of rainfall, which in the south of China (Haikou, Hong Kong) is about 2.5$^{o}/_{oo}$ more negative than in the Bay of Bengal (Yangoon). Strong seasonal variations of the deuterium excess values in precipitation observed in some areas of the studied region result from a complete reversal of atmospheric circulation over these areas and changing source of atmospheric moisture. High d-excess values observed at Tokyo and Pohang during winter (15-25$^{o}/_{oo}$) result from interaction of dry air masses from the northern Asian continent passing the Sea of Japan and the China Sea and picking up moisture under reduced relative humidity. The isotopic composition of precipitation also provides information about the maximum extent of the ITCZ on the continent during summer.

1. Introduction

The concentrations of deuterium and oxygen-18 in meteoric waters exhibit a broad range of variations, both in time and space. Present-day distribution patterns of these isotopes in global precipitation reveal a close linkage with some climatically relevant meteorological parameters, such as surface air temperature, relative humidity of the atmosphere, and amount of precipitation [e.g., *Dansgaard,* 1964; *Yurtsever and Gat,* 1981; *Rozanski et al..,* 1993]. These empirical relations were used in numerous studies aimed at reconstructing past climates from various environmental archives, such as ice cores, lacustrine deposits, tree cellulose, and others [e.g., *Johnsen et al.* 1989, *Edwards,* 1993; *Thompson et al.,* 1989; *Gasse and van Campo,* 1994]. Whereas the link between isotope signature of precipitation and climate at mid latitudes and high latitudes is in general well understood, this is much less the case for the tropics.

A considerable amount of theoretical and applied work carried out during the past 3 decades was devoted to a better characterization of the processes controlling the isotopic evolution of meteoric waters at different levels of the global hydrological cycle. It has been demonstrated that spatial and temporal variations of ^{2}H and ^{18}O isotope composition of precipitation have their origin in isotope fractionation effects accompanying evaporation of water from the ocean and subsequent condensation of water vapor during its atmospheric transport. It became apparent that the isotopic composition of local precipitation, in particular, at mid latitudes and high latitudes, is controlled by regional-scale processes, i.e., by average parameters of the evaporation process at source regions of atmospheric moisture and by average water vapor transport patterns into the continents and the resulting "rain-out history" of the air masses precipitating at a given place [e.g., *Dansgaard,* 1964; *Craig and Gordon,* 1965; *Merlivat and Jouzel* 1979;

[1] Now at Amatosa Ingenieria, S.L. Madrid, Spain and CEDEX, Ministry of Public Works, Madrid, Spain.

Paper number 98JD02582.
0148-0227/98/98JD-02582$09.00

Rozanski et al., 1982; *Siegenthaler and Matter*, 1983; *Johnsen et al.*, 1989, *Ingraham and Craig*, 1993; *Charles et al.*, 1994].

Since 1961, the International Atomic Energy Agency (IAEA) in cooperation with the World Meteorological Organization (WMO), has been conducting a worldwide survey of the isotopic composition of monthly precipitation (tritium, deuterium, oxygen-18). The program was launched with the primary objective of collecting systematic data on isotope content of precipitation on a global scale, characterizing their spatial, and temporal variability and, consequently, providing basic isotope data for the use of environmental isotopes in hydrogeological investigations. It soon became apparent that the collected data are also useful in other water-related fields, such as oceanography, hydrometeorology, and climatology. The IAEA/WMO Global Network "Isotopes in Precipitation" (GNIP) is being run as a collaborative effort of numerous institutions and individuals, under the general coordination and guidance of the IAEA. The IAEA carries out isotope analyses of about 30% of the collected samples and maintains the GNIP database.

This paper is focused on spatial and temporal variability of the stable isotope composition of precipitation in the southeast Asia and western Pacific region, with special emphasis on the China territory (Figure 1). Other regional surveys of this type, largely based on the GNIP database, have been published [e.g., *Salati et al.*, 1979; *Gonfiantini*, 1985; *Joseph et al.*, 1992; *Rozanski and Araguás-Araguás*, 1995; *Rozanski et al.*, 1996]. This survey concentrates on data available for 29 precipitation collection sites in the China territory, including 10 stations that were established in 1988 as a part of the IAEA/WMO global network [IAEA, 1969, 1970, 1971, 1973, 1975, 1979, 1983, 1986, 1990, 1994, 1992]. Selected stations representing adjacent regions, especially those which began collection of monthly precipitation for isotope analyses in the early 1960s (e.g. Hong Kong, Tokyo, Bangkok, New Delhi) are also included in the discussion. The geographical distribution of the meteorological stations discussed in this paper is shown in Figure 1.

By convention, the measured ratios of the stable hydrogen and oxygen isotopes in water samples ($^2H/^1H$ and $^{18}O/^{16}O$, respectively) are expressed as parts per thousand of their deviation relative to the standard V-SMOW (Vienna Standard Mean Ocean Water). These so-called delta values, δ^2H or $\delta^{18}O$, respectively, are thus defined by the following equation (in per mil):

$$\delta = (R_{SAMPLE}/R_{STANDARD} - 1)\times 1000 \quad (1)$$

where R_{SAMPLE} and $R_{STANDARD}$ stand for the isotope ratios $^2H/^1H$ and $^{18}O/^{16}O$ of the sample and the standard, respectively. Typical uncertainties involved in isotope analysis of individual precipitation samples reported in this paper are of the order of $1^0/_{00}$ and $0.1^0/_{00}$ for δ^2H and $\delta^{18}O$, respectively.

2. Atmospheric Circulation and Climate of the Region

The meteorology and especially the pluviometric regime of the southeast portion of the Asian continent is dominated by the influence of five major air masses [*Ren*, 1985; *Bryson*, 1986; *Winkler and Wang*, 1993]: (1) polar air mass originating in the Arctic, (2) continental air mass originating over central Asia, (3) tropical-maritime air mass originating in the northern Pacific, (4) equatorial-maritime air mass originating in the western equatorial Pacific, and (5) equatorial-maritime air mass originating in the Indian Ocean. The maximum extent of these air masses is schematically shown in Figure 1. The relative importance of different air masses over the region in the course of a year is modulated by the monsoon activity and the seasonal displacement of the Intertropical Convergence Zone (ITCZ). The ITCZ stays around 15°S in January and moves in July as far as 40°-45°N, in a relatively narrow band between 120°E and 140°E [Perry and Walker, 1977].

The Tibetan Plateau plays a central role in the regional climatology. It blocks the mid latitude westerlies and splits the jet that moves to the north and the south of the plateau. Cooling of the air masses over the plateau results in the formation of a central Asian airstream which dominates western and northwestern China with varying intensity throughout the year. A characteristic feature of the regional climate is a complete reversal of weather patterns from summer to winter [*Bryson*, 1986]. The low pressure over the plateau during summer is centered at about 70°-80°E and induces a supply of moist, warm air from the Indian and Pacific Oceans to the continent (summer monsoon) from about June through August. In winter, a high-pressure ridge is centered at about 80°-90°E over the Tibetan Plateau and cold, dry air moves out of the plateau to the north, east, and south (winter monsoon), from about October through April. The transition in atmospheric circulation takes place in May and September.

The discussed region encompasses a wide spectrum of climates: from arid and semiarid continental climate in North West China and Mongolia (annual precipitation less than 200 mm), tropical, monsoon-type climate in India, southeast China, and Indonesia, to tropical humid climate of equatorial Pacific with annual rainfall exceeding 2,300 mm. A wide range of altitudes is represented by the analyzed sites: from sea level to an elevation of 3,649 m above sea level (Lhasa station on the Tibetan Plateau). Also, they cover a broad range of annual mean surface air temperatures, from -1.5°C (Enisejsk) to 28.1°C (Tarawa, Bangkok). The seasonal amplitude of temperature varies for the analyzed sites from around 40°C for Enisejsk to less than 1°C for Tarawa.

3. Long-Term Averages of Isotope and Meteorological Parameters

The isotope and meteorological data gathered by the stations operating in the region are summarized in Tables 1 and 2. The stations are grouped according to five major moisture source regions mentioned above. The long-term annual weighted means of δ^2H, $\delta^{18}O$, and deuterium excess values ($d = \delta^2H - 8\times\delta^{18}O$), as well as the annual means of surface air temperature and the amount of rainfall for the analyzed stations are reported in Table 1. Weigthing was performed with respect to the amount of precipitation.

The spatial distribution of the annual mean $\delta^{18}O$ values is shown in Figure 2 (top). Although the overall time period covered by the data exceeds 30 years, actually only few stations were run longer than a decade. The number of available monthly $\delta^{18}O$ data is reported in parentheses in Table 1. Asterisks indicate the stations with poor data coverage (less than 1 calendar year). The calculated weighted mean $\delta^{18}O$ and δ^2H values for those stations should be treated with caution.

Table 2 summarizes the long-term seasonal averages of isotope and meteorological data available for the analyzed stations. The averages were calculated for summer and winter seasons (wet and dry periods in some areas), with slightly varying duration from region to region, according to the varying seasonal distribution of rainfall. For stations with bimodal distribution of rainfall the averages were calculated respectively for three periods. As in Table 1, seasonal weighted averages of δ^2H, $\delta^{18}O$, and the deuterium-excess value were calculated. Figure 2 (bottom) shows spatial distribution of the seasonal average $\delta^{18}O$ values for the rainy period, during the operation of the Asian monsoon.

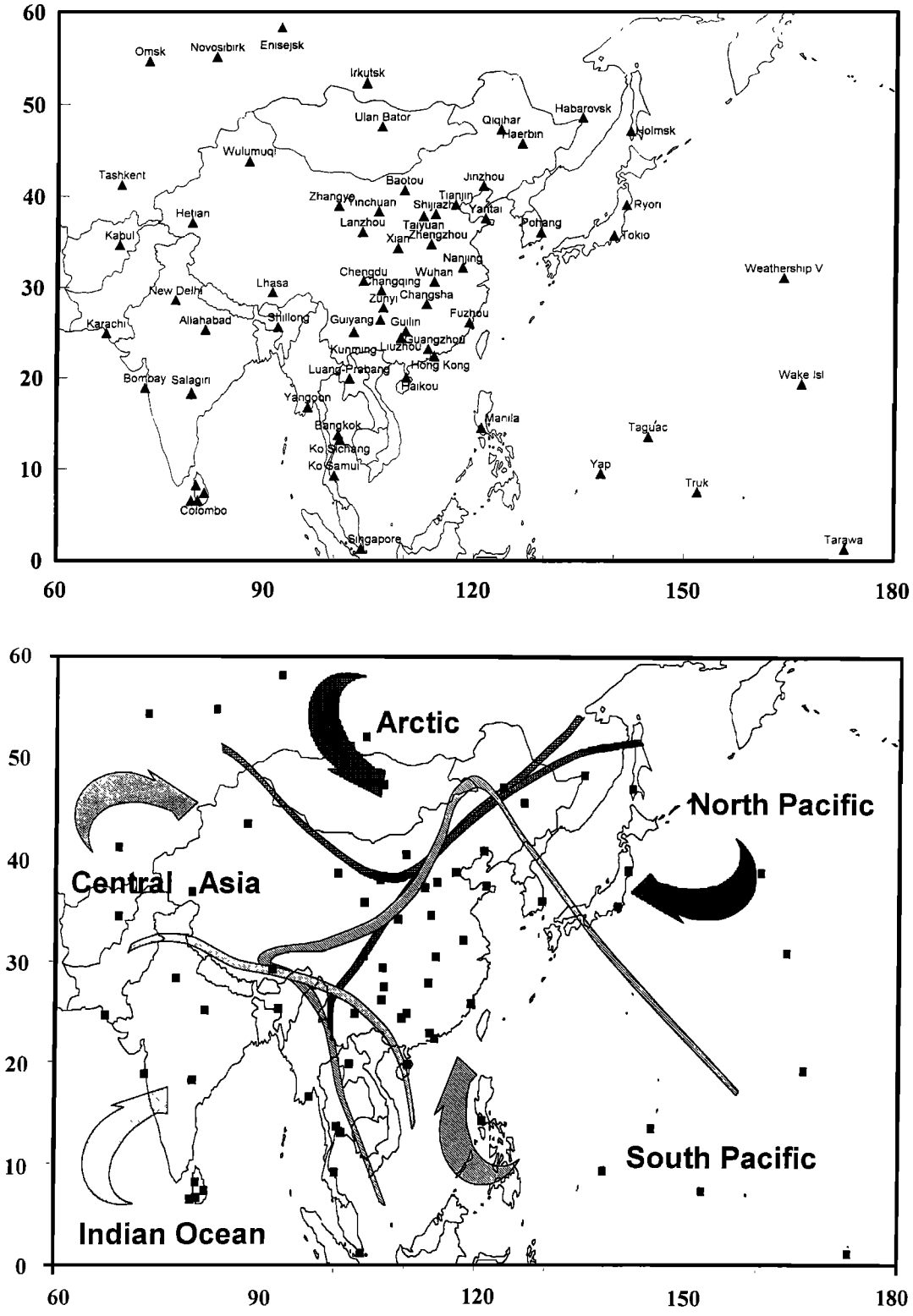

Figure 1. (top) Geographical distribution of stations in the southeast Asia and western Pacific region, contributing to the database of the International Atomic Energy Agency/World Meteorological Organization Global Network of Isotopes in Precipitation (GNIP). (bottom) Schematic representation of the maximum extent of major air masses controlling weather patterns and rainfall regime in the study area [after *Bryson*, 1986, *Winkler and Wang*, 1993].

The magnitude of the deuterium excess is controlled mainly by the relative humidity over the evaporating surface, the sea surface temperature, and the wind speed at the source region of atmospheric moisture [*Merlivat and Jouzel*, 1979]. The d values close to $+10^{0}/_{00}$ are observed in most continental waters, at present [*Craig*, 1961, *Yurtsever and Gat*, 1981; *Rozanski et al.*, 1993]. The deuterium excess of snow may vary in response to changes of the supersaturation of vapor with respect to temperature of snow formation [*Jouzel and Merlivat*, 1984; *Fisher*, 1991; *Petit et al*, 1991]. However, this process is

Table 1. Summary of Isotope and Meteorological Data for 61 Stations of the International Atomic Energy Agency/ World Meteorological Organization Network for "Isotopes in Precipitation" (GNIP) located in the Southeast Asia and Adjacent Regions.

Station Name	Location	Altitude, masl	Annual Precipitation, mm	Mean Annual Temperature, °C	$\delta^{18}O_w$, ‰	$\delta^{2}H_w$, ‰	*d*-excess, ‰
			South Pacific Domain				
Tarawa	172.92°E, 1.35°N	4	2391	28.1	-6.23 (17)	-38.5	11.3
Truk	151.85°E, 7.47°N	2	3582	27.4	-5.31 (93)	-32.2	10.2
Yap	138.09°E, 9.49°N	0	2812	27.1	-5.67 (99)	-34.3	9.6
Taguac	144 83°E, 13.55°N	110	2659	25.9	-5.08 (112)	-30.6	10.8
Manila	121.00°E, 14.52°N	14	1957	26 9	-6.74 (48)	-44.2	9.8
Singapore	103.90°E, 1.35°N	32	2164	26.3	-7.29 (97)	-46.9	13.2
Ko Samui	100.03°E, 9.28°N	7	1539	27.8	-5.75 (36)	-27.7	10.5
Ko Sichang	100.80°E, 13.17°N	0	1133	28.0	-6.16 (46)	-38.9	10.1
Bangkok	100.50°E, 13.73°N	2	1452	28.1	-6.62 (240)	-44.0	9.0
Haikou	110.21°E, 20.02°N	15	1658	25.3	-6.62 (33)	-42.1	10.9
Luang -Prabang	102.13°E, 19.88°N	305	1229	25.7	-7.49 (26)	-50.9	9.0
Kunming	102.68°E, 23.02°N	1841	942	15.0	-10.42 (67)	-73.2	10.2
Lhasa	91.08°E, 29.42°N	3649	425	8.0	-15.25 (42)	-112.0	9.9
Hong-Kong	114.17°E, 22.32°N	65	2190	22.9	-6.46 (262)	-41.1	10.3
Guangzhou	113.32°E, 23.13°N	7	1724	22.2	-5.90 (30)	-41.0	6.2
Nanjing	118.18°E, 32.18°N	26	1108	14.6	-8.41 (58)	-54.9	12.3
Fuzhou	119.17°E, 26.05°N	16	1341	20.0	-6.40 (71)	-40.9	9.9
Changsha	113.04°E, 28.12°N	37	1271	17.2	-5.65 (57)	-32 1	13.0
Guilin	110.08°E, 25.07°N	170	1531	19.0	-6.13 (92)	-35.5	14.8
Guiyang	106.43°E, 26.35°N	1071	974	15.3	-8.33 (58)	-52.2	14.4
Liuzhou	109.40°E, 24.35°N	97	1041	20.9	-6.43 (53)	-43.5	7.9
Wuhan	114.13°E, 30.62°N	23	1051	16.4	-6.61 (23)	-42.8	10.1
Zunyi	106.88°E, 27.70°N	844	978	15.4	-8.40 (74)	-55.2	11.7
Chengdu	104.02°E, 30.67°N	506	888	15.7	-7.45 (45)	-53 6	6.0
Changqing *	106.60°E, 29.62°N	192	-----	------	-10.41 (5)	-69.6	13.7
			North Pacific Domain				
Weathership V	164.00° E, 31.00°N	0	932	19 1	-4.34 (96)	-23.9	10.3
Wake Island	166.65° E, 19.28°N	3	908	26.6	-2.18 (151)	-9.6	7.6
Ryori	141.50° E, 39.02°N	260	1265	9.9	-8.37 (86)	-54.5	12.4
Tokyo	139.77 °E, 35.68°N	4	1378	15.5	-7.30 (219)	-46 3	11.3
Jinzhou*	121.10° E, 41.13°N	66	540	9 4	-7.49 (12)	-54 5	5.4
Pohang	129.38° E, 36.03°N	6	1106	13.1	-7 76 (110)	-51.0	10.1
Yantai	121.40° E, 37.53°N	47	563	12.9	-7.24 (44)	-50.8	7 1
Tianjin	117.10° E, 39.06°N	3	469	13.2	-7.66 (45)	-50.9	10.4
Shijiazuang	114.25° E, 38.02°N	80	551	13.1	-7 83 (76)	-56.0	6.6
Taiyuan	112.55° E, 37 78°N	778	415	10.3	-8.50 (20)	-61.0	7.0
Zhengzhou	113.65° E, 34 72°N	110	536	14.2	-7.59 (57)	-54.2	6.5
Xian	108.93° E, 34.30°N	397	519	13.5	-7.49 (60)	-49.1	10.8
Haerbin	126.62° E, 45.68°N	172	484	4.9	-10.10 (26)	-74 6	6.2
			Indian Ocean Domain				
Colombo*	79.52° E, 6.54° N	5	2397	26.9	-2.67 (11)	-11.5	9.9
Salagiri*	79.44° E, 6.54° N	550	760	25.8	-5.04 (5)	-33.4	7.0
Bombay	72.82° E, 18.90° N	10	1939	27.3	-1.51 (50)	-3.7	8 8
Karachi	67.13° E, 24.90° N	23	195	25.7	-3.80 (45)	-22.9	8.3
New Delhi	77.20° E, 28.58° N	212	784	25.0	-5.70 (260)	-36.6	8.5
Allahabad*	81.44° E, 25.27° N	98	1032	26.1	-7.36 (5)	-51.0	7.8
Shillong	91.88° E, 25.57° N	1598	2156	17.5	-3.67 (31)	-28.5	10.8
Yangoon	96.17° E, 16.77° N	20	2399	27.2	-4.34 (20)	-28.9	5.8
			Central Asia Domain				
Kabul	69.08° E, 34.67° N	1860	330	11.6	-7.15 (109)	-37.5	18.6
Tashkent*	69.27° E, 41.27° N	428	469	13.6	-7.00 (7)	-42.9	13.1
Omsk*	73.24° E, 54.56° N	94	401	7.6	-13.46 (8)	-98.2	8.9
Hetian	79.56° E, 37.08° N	1375	210	8.2	-5.47 (47)	-32.6	11.1
Wulumiqi	87.62° E, 43.78° N	918	287	6.9	-10.84 (72)	-74.6	12.2
Zhangye	100.43° E, 38.93° N	1483	123	7.5	-6.33 (52)	-41.6	9.1
Novosibirk*	82.90° E, 55.03° N	162	422	0.9	-14.64 (12)	-104.0	12.8
Enisejsk*	92.09° E, 58.27° N	98	491	-1.5	-13.29 (12)	-98.4	7 9

Table 1 (continued)

Station Name	Location	Altitude, masl	Annual Precipitation, mm	Mean Annual Temperature, °C	$\delta^{18}O_w$, ‰	$\delta^{2}H_w$, ‰	*d*-excess, ‰
			Arctic Domain				
Irkutsk	104.35° E, 52.27° N	485	445	0.0	-12 12 (14)	-92.9	4.1
Ulan Bator*	106.59° E, 47.56° N	1338	240	0.3	------ (7)	------	------
Baotou	109.85° E, 40.67° N	1067	284	7 5	-7.78 (61)	-55.3	7 0
Yinchuan	106.13° E, 38.29°N	1112	205	8.9	-6.62 (28)	-43.8	9.1
Lanzhou	103.88° E, 36.05° N	1517	296	10.0	-6.18 (16)	-36.4	13.1
Qiqihar	123.55° E, 47.23° N	147	581	4.3	-10 61 (50)	-79 5	5.3
Habarovsk*	135 17° E, 48 52° N	72	647	1 6	-14.29 (11)	-103.0	11 4

The summary covers the time period 1961-1993. The stations are grouped according to major source areas of moisture-producing precipitation in the region. The isotope data are reported as per mil deviations from the standard Vienna standard Mean Oceanic Water (V-SMOW). For calculation of the weighted means, weighting by amount of precipitation has been adopted The number of available monthly $\delta^{18}O$ data is reported in parentheses.

* Stations had poor data coverage (equal to or less than 1 calendar year). The calculated weighted mean $\delta^{18}O$ and $\delta^{2}H$ values for these should be treated with caution.

important only in low-temperature environments (polar regions). Under conditions of low relative humidity and in cases of light rainfall, especially in arid and semiarid climates, partial evaporation of raindrops below the cloud base may substantially reduce the *d* value of raindrops collected at the ground-level, when compared with the in-cloud conditions.

The regional $\delta^{2}H$ - $\delta^{18}O$ relationship, based on the annual weighted means of $\delta^{2}H$ and $\delta^{18}O$ for the stations listed in Table 1, is shown in Figure 3. The data points define a regional line which is practically indistinguishable from the Global Meteoric Water Line ($\delta^{2}H = 8\times\delta^{18}O + 10$), although some stations clearly lie off the line, exhibiting significantly higher (e.g., Kabul and Guiyang) or lower (e.g., Irkutsk and Qiqihar) *d* values.

4. Monsoon Control of Stable Isotope Composition of Precipitation

Two monsoon systems operate during summer in the southern part of the region: the Indian monsoon originating in the Indian Ocean and the Pacific monsoon originating in the western equatorial Pacific (Figure 1). Monsoon rains reveal a distinct isotope signature: they are usually more depleted in ^{2}H and ^{18}O than winter rains on the same area, in spite of generally higher summer temperatures. The influence of the surface air temperature on the overall isotopic fractionation during precipitation is overshadowed by the effects controlled by the amount of precipitation. The difference between the isotopic composition of summer and winter rains increases if one moves inland along the monsoon track. The extreme situation occurs at Lhasa station, for which the difference between winter and summer average $\delta^{18}O$ reaches 6.3‰, with temperatures of 4.6°C and 15.0°C for winter and summer, respectively (see Table 2). Surface air temperature becomes the main controlling factor in the northern part of the region, far from areas influenced by monsoon activity. There, the seasonal trend of $\delta^{2}H$ and $\delta^{18}O$ is reversed, with precipitation enriched in heavy isotopes in summer and depleted in winter. This situation is illustrated in Figure 4 which shows spatial distribution of the difference between weighted mean $\delta^{18}O$ values for the summer and winter season (rainy and dry period, respectively). Positive values of this difference indicate the sites with prevailing control of temperature, whereas negative values indicate those areas where monsoon control is dominating. It is worth noting that the line separating these two types of stations (positive and negative values of $\Delta\delta^{18}O$, respectively) closely matches the maximum extent of ITCZ over the continent during boreal summer.

Owing to the topographic barrier of the main Himalayan chain, the Indian monsoon can enter the Tibetan Plateau only through its southeast corner, along the valleys of major rivers (Nu Shang, Yun Ling, and Chang Jiang). There is also a limited possibility that some moisture can enter the plateau through the Brahmaputra Valley. The chain of Himalaya mountains effectively blocks the direct northward transport of moisture. The main source of moisture for the Tibetan Plateau is the Pacific monsoon.

The two monsoon systems differ substantially with respect to the initial isotopic composition of atmospheric moisture entering the continent. Summer rains in the Gulf of Bengal, controlled by the Indian monsoon, are relatively enriched in both ^{2}H and ^{18}O; the average $\delta^{18}O$ of rainfall is around -4.5‰ in Yangoon. Similar values are expected for the Calcutta region, based on the isotopic composition of shallow groundwater there [*Krishnamurthy and Bhattacharya*, 1991]. These relatively high values suggest proximity to the source of vapor (Gulf of Bengal?) and/or only a minor reduction of the initial moisture load of air masses along the oceanic portion of the monsoon track. On the other hand, precipitation in the region of the China Sea and the Gulf of Tonkin, belonging to the Pacific monsoon domain, is isotopically more depleted; the average weighted mean $\delta^{18}O$ is equal to -8.1‰ for Haikou and -6.5‰ for Hong Kong. The available data suggest that rainfalls belonging to the given monsoon system have also distinct *d* values; summer rainfall at Yangoon has an average *d*-excess around 6‰, whereas Hong Kong and Haikou reveal for the same period substantially higher values (9.9‰ and 11‰, respectively).

The extreme isotope depletion of rainfall observed at Lhasa station during the summer months (July and August) was modelled using the "isolated air mass" approach based on the Rayleigh condensation process with immediate removal of precipitation from the cloud [e.g., *Dansgaard* 1964; *Siegenthaler and Matter,* 1983; *Van der Straaten and Mook,* 1983; *Gedzelman,* 1988; *Johnsen et al.*, 1989]. The progressive depletion in ^{18}O of rainfall along a presumable trajectory of the Pacific monsoon reaching the Tibetan Plateau was calculated using the Rayleigh formula (see Table 3). Four stations were considered: Haikou and Hong Kong, representing moist air masses entering the continent; Kunming, located halfway to the Tibetan Plateau; and Lhasa. The rain-out factor *F* was calculated as a ratio of total precipitable water in the atmosphere over the continent to that observed in the coastal region. The total water content in the atmosphere above the stations during the analyzed time period was derived from aerological data reported by

Table 2. Summary of Seasonal Weighted Averages of Isotope and Meteorological Data for the Analyzed Stations of the Region.

Station Name	Period	Precipitation Amount, mm	Mean Air Temperature, °C	$\delta^{18}O_w$, ‰	$\delta^{2}H_w$, ‰	*d*-excess, ‰	$\Delta\delta^{18}O$, ‰
			South Pacific Domain				
Tarawa	April-Oct.	1171 (49)	28.1	-6.06	-37.9	10.6	0.64
	Nov.-May	1201 (51)	28.2	-5.42	-31.2	12.2	
Truk	April-Oct.	2380 (66)	27.4	-5.64	-35.4	10.1	-1.78
	Nov.-March	1200 (34)	27.5	-3.86	-21.0	9.3	
Yap	May-Oct.	1638 (58)	27.1	-6.04	-34.6	10.6	-1.88
	Nov.-April	1175 (42)	27.1	-4.16	-24.5	7.5	
Taguac	May-Oct.	1744 (66)	26.2	-5.56	-33.8	10.9	-3.19
	Nov.-April	915 (34)	25.6	-2.37	-10.0	9.1	
Manila	May-Oct.	1751 (90)	27.6	-6.68	-43.9	9.5	-1.71
	Nov.-April	197 (10)	26.3	-4.97	-31.5	8.0	
Singapore	Sept.-Dec	1244 (57)	26.4	-6.25	-39.6	12.8	-1.93
	Jan.-Aug	922 (43)	26.0	-8.18	-53.8	13.0	
Bangkok	May-Oct.	1304 (88)	28.6	-6.62	-44.4	8.9	-3.71
	Nov.-April	177 (12)	27.7	-2.91	-17.1	8.3	
Haikou	May-Sept.	881 (56)	30.0	-8.06	-53.5	11.0	-3.75
	Oct.-April	697 (44)	22.0	-4.31	-22.9	11.5	
Luang –Prabang	May-Sept.	964 (78)	28.1	-8.28	-58.3	8.0	-3.99
	Oct.-April	265 (22)	24.0	-4.29	-25.1	9.2	
Kunming	May-Oct.	839 (89)	18.5	-10.49	-73.5	10.4	-5.21
	Nov.-April	103 (11)	11.5	-5.28	-32.3	9.9	
Lhasa	June-Sept.	377 (90)	15.0	-16.63	-124.7	8.4	-6.27
	Oct.-May	42 (10)	4.6	-10.36	-66.2	16.7	
Hong-Kong	May-Sept.	1678 (76)	27.7	-6.69	-43.6	9.9	-3.18
	Oct.-April	518 (24)	19.4	-3.51	-17.3	10.5	
Guangzhou	May-Sept.	1241 (72)	27.7	-6.32	-44.2	6.3	-2.96
	Oct.-April	484 (28)	18.3	-3.36	-19.4	7.5	
Nanjing	June-Sept.	712 (60)	23.8	-9.36	-63.9	11.0	-3.46
	Oct.-Feb.	217 (18)	7.0	-6.90	-39.2	16.0	
	March-May	264 (22)	14.3	-4.91	-24.7	14.6	
Fuzhou	June-Sept.	633 (45)	28.0	-7.21	-51.2	6.5	-2 11
	Oct.-Feb.	233 (17)	15.3	-5.32	-24.9	12.7	
	March-May	529 (38)	18.1	-4.84	-25.8	13.0	
Changsha	June-Sept.	463 (36)	27.5	-8.20	-55.9	9.8	-4.35
	Oct.-Feb.	325 (26)	10.1	-4.88	-24.1	15.0	
	March-May	482 (38)	15.3	-2.89	-8.4	14.7	
Guilin	May-Sept.	901 (59)	26.6	-7.58	-47.2	13.5	-4.17
	Oct.-April	631 (41)	13.7	-3.41	-12.7	16.1	
Guiyang	May-Oct	737 (76)	21.7	-9.14	-60.1	13.0	-5.32
	Nov.-April	227 (24)	8.9	-3.82	-11.3	19.2	
Liuzhou	May-Sept.	585 (56)	27.8	-7.79	-56.0	6.4	-4.26
	Oct -April	458 (44)	16.0	-3.53	-23.1	5.1	
Wuhan	June-Sept.	579 (50)	25.9	-8.95	-66.2	5.4	-4.62
	Oct.-Feb.	214 (18)	8.8	-6.44	-39.1	12.4	
	March-May	374 (32)	16.2	-3.15	-11.6	13.6	
Zunyi	May-Oct.	770 (79)	21.6	-8.92	-60.9	10.3	-4.72
	Nov.-April	209 (21)	9.3	-4.20	-20.4	13.2	
Chengdu	May-Sept.	762 (86)	22.5	-7.40	-53.2	6.0	-3.78
	Oct.-April	127 (14)	10.9	-3.62	-23.8	5.2	
			North Pacific Domain				
Weathership V	Oct.-March	580 (62)	17.0	-3.89	-20.4	10.9	0.32
	April-Sept.	356 (38)	21.2	-4.21	-26.1	7.3	
Wake Island	July-Oct.	499 (55)	27.9	-2.56	-12.9	7.5	-1.59
	Nov.-June	411 (45)	25.9	-0.97	0.3	7.9	
Ryori	May-Sept.	730 (57)	17.6	-7.97	-53.7	9.6	0.40
	Oct.-April	545 (43)	4.5	-8.37	-51.5	15.7	
Tokyo	May-Sept.	741 (54)	7.3	-6.70	-45.8	7.3	0.52
	Oct.-April	637 (46)	16.1	-7.22	-41.5	16.1	
Jinzhou*	May-Sept.	455 (84)	20.9	-7.24	-53.9	4.0	-------
	Oct.-April	85 (16)	1.2	-------	-------	------	

Table 2 (continued)

Station Name	Period	Precipitation Amount, mm	Mean Air Temperature, °C	$\delta^{18}O_w$, ‰	$\delta^{2}H_w$, ‰	*d*-excess, ‰	$\Delta\delta^{18}O$, ‰
Pohang	May-Sept.	735 (66)	21.7	-8.14	-55.2	8.1	-1.45
	Oct.-April	372 (34)	7.0	-6.69	-38.4	14.3	
Yantai	May-Sept.	429 (76)	22.2	-6.99	-51.0	4.9	-0.29
	Oct.-April	138 (24)	6.2	-6 70	-41.9	11.7	
Tianjin	May-Sept.	436 (85)	25.5	-7.40	-49.5	9.7	-1.06
	Oct.-April	78 (15)	6.2	-6.34	-38.9	11.8	
Shijiazuang	May-Sept.	430 (78)	23.7	-7.24	-52.9	4.9	0.51
	Oct.-April	120 (22)	5.6	-7.75	-51.9	10.1	
Taiyuan	May-Sept.	359 (87)	20.3	-7.13	-51.5	5.5	0.84
	Oct.-April	56 (13)	3.1	-7.97	-56.9	6.9	
Zhengzhou	May-Sept.	378 (68)	24.0	-7.00	-53.7	2.3	-1.06
	Oct.-April	179 (32)	7.1	-5.94	-40.6	6.8	
Xian	May-Sept.	391 (72)	23.2	-7.39	-50.4	8.7	-0.36
	Oct.-April	155 (28)	6.6	-7.03	-45.2	11.1	
Haerbin	May-Sept.	466 (85)	18.5	-9.54	-71.3	5.1	-0.20
	Oct.-April	83 (15)	-5.1	-9.34	-67.5	7.3	
			Indian Ocean Domain				
Bombay	Jun-Sept.	1885 (95)	27.9	-1.33	-2.4	8.8	2.35
	Oct.-May	99 (5)	27.1	-3.68	-22.4	7.0	
New Delhi	June-Sept.	670 (84)	30.8	-5.85	-37.7	8.0	-4.32
	Oct.-May	123 (16)	22.1	-1.53	-5.9	6.0	
Shillong	May-Oct.	1800 (84)	20.3	-6.87	-43.9	11.1	-5.69
	Nov.-April	355 (16)	14.6	-1.18	-7.4	12.3	
Yangoon	May-Oct.	2296 (95)	27.5	-4.54	-30 1	6.2	-0.62
	Nov.-April	133 (5)	27 0	-3.92	-27 9	3 4	
			Central Asia Domain				
Kabul	Oct.-April	291 (88)	5.0	-7.91	-45.0	18.8	-6.51
	May-Sept.	41 (12)	20.9	-1.40	6.5	11.4	
Hetian	May-Sept.	163 (78)	18.5	-1.91	-5.1	10.2	12.75
	Oct.-April	45 (22)	2.0	-14.66	-111.5	5.7	
Wulumiqi	May-Sept.	161 (56)	20.3	-6.88	-47.2	7.9	9.01
	Oct.-April	127 (44)	-2 6	-15.89	-111.2	15 9	
Zhangye	May-Sept.	99 (75)	18.3	-4.22	-28.4	5.4	8.37
	Oct.-April	33 (25)	-0.3	-12.59	-90.0	10.7	
Novosibirk*	May-Oct.	295 (70)	12.2	-12.49	-85 8	14.1	6.68
	Nov.-April	128 (30)	-10.1	-19.17	-142.3	11.1	
Enisejsk*	May-Oct.	312 (64)	10.4	-11.86	-84.8	10.1	5 78
	Nov.-April	177 (36)	-12.8	-17.64	-138.3	2.8	
			Arctic Domain				
Irkutsk	May-Oct.	376 (82%)	11.1	-11.65	-90.3	3.0	4.48
	Nov.-April	84 (18%)	-10.9	-16.13	-122.9	6.2	
Baotou	May-Sept.	231 (81%)	19.6	-6.88	-49.7	5.4	3.38
	Oct.-April	53 (19%)	-1.2	-10.26	-68.1	13.2	
Yinchuan	May-Sept.	169 (76%)	20.0	-5.60	-36 5	8.3	3 27
	Oct.-April	52 (24%)	1.0	-8.87	-56.3	14.7	
Lanzhou	May-Sept.	276 (85%)	19.1	-5.04	-29.7	10.6	5.43
	Oct.-April	47 (15%)	3.1	-10 47	-68.4	15.4	
Qiqihar	May-Sept.	460 (86%)	18.2	-9.40	-71.2	3.9	7.37
	Oct.-April	77 (14%)	-5.9	-16.77	-122.3	11.9	

Periods of averaging vary slightly from station to station, depending on the duration of the rainy period. The fraction of annual rainfall used for isotope analyses is reported in parentheses (in percent) The difference $\delta^{18}O_{SUMMER} - \delta^{18}O_{WINTER}$ (weighted averages) is reported in the last column.

* These stations had poor coverage.

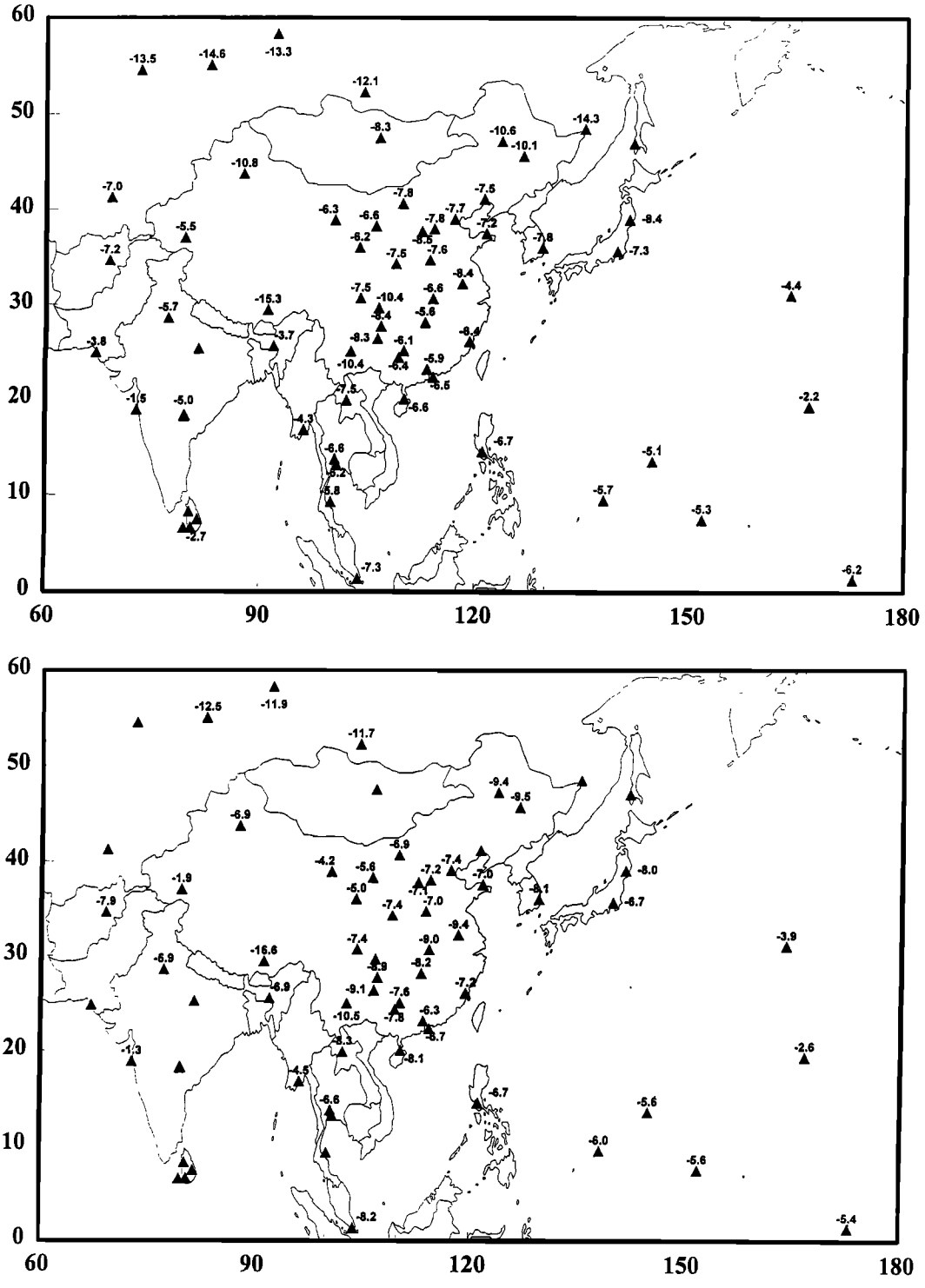

Figure 2. (top) Spatial distribution of annual weighted mean $\delta^{18}O$ values in precipitation at the stations of the region. Weighting was performed with respect to the amount of precipitation. (bottom) Spatial distribution of weighted mean $\delta^{18}O$ representing the major rainy period at the analyzed stations (see Table 2). Weighting was performed with respect to the amount of precipitation.

Kuznetsova [1990]. The effective condensation temperature was assumed to be equal to the measured ground level temperature. As can be seen from Table 3, even this highly simplified approach leads to $\delta^{18}O$ values along the monsoon track that are in good agreement with the observed ^{18}O isotope composition of rainfall, thus confirming the dominating role of the rain-out effect in controlling isotopic composition of monsoon precipitation.

5. Isotope Indicators of Seasonal Changes of Circulation Patterns

The factors controlling seasonal variability of the isotopic composition of precipitation in the region are summarized in Table 4. The slopes of the relationships $\delta^{18}O$/temperature and $\delta^{18}O$/precipitation amounts are derived from a linear fit of the

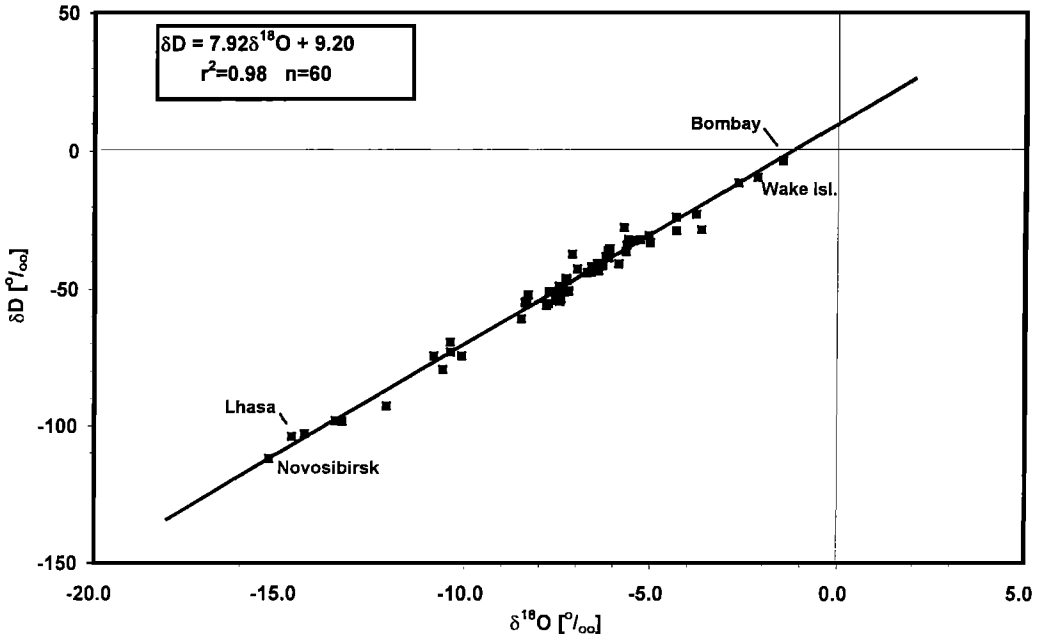

Figure 3. Regional δ^2H - $\delta^{18}O$ relationship based on the annual weighted mean δ^2H and $\delta^{18}O$ values for the analyzed stations of the region.

corresponding long-term monthly means. Numerical values are reported only for those stations for which the correlation coefficient r is larger than 0.50. The slope and the intercept of the Local Meteoric Water Line (LMWL) derived from the least squares fit of the monthly $\delta^{18}O$ and δ^2H data available for the given station are also included in Table 4. It is apparent from these data and the schematic presentation in Figure 5 that the climatic sensitivity of the isotopic signal in precipitation varies considerably: $\delta^{18}O$ and δ^2H of rainfall in the northern part of the region (above approximately 35°N) are mainly controlled by temperature; in the southern and southeastern part they are dominated by the precipitation amount effect. There is also a number of sites where neither of these two parameters has a statistically significant correlation with the isotopic composition

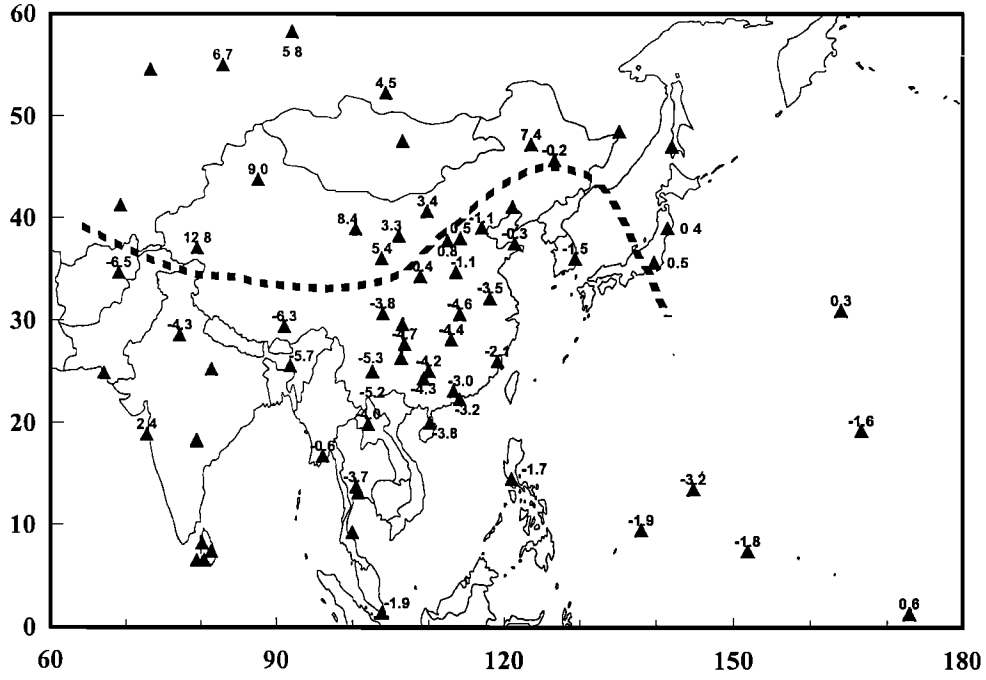

Figure 4. Spatial distribution of the difference $\delta^{18}O_{SUMMER}$ - $\delta^{18}O_{WINTER}$ for the analyzed stations of the region. The seasonal averages are weighted means (weighting by the amount of precipitation). The dashed line separates the areas of positive and negative values of the difference, and coincides with the maximum extent of the Intertropical Convergence Zone (ITCZ) in the region during summer.

Table 3. Comparison of Measured and Calculated $\delta^{18}O$ Values of Rainfall Along the Trajectory of Pacific Monsoon, From the South of China to Lhasa, Tibetan Plateau, July to August.

Station	Mean Temperature, °C	Total Precipitable Water, mm	Rain-out Factor, F	$\delta^{18}O$ Measured, ‰	$\delta^{18}O$ Calculated,* ‰
Haikou/Hong Kong, weighted mean	30.2	65	1.00	-7.2	-----
Kunming	19.4	36	0.55	-12.7	-12.0
Lhasa	15.2	18	0.28	-18 3	-18.7

* The isotopic composition of rainfall δ_R at the given site was calculated using the Rayleigh-type formula: $\delta_R=(\alpha/\alpha_{RO})(\delta_{RO}+1)F^{(\alpha-1)}-1$, where α is the equilibrium fractionation factor during formation of rainfall at the effective condensation temperature T; $(\delta_{RO}+1)=\alpha_{RO}(\delta_{VO}+1)$ is the isotopic composition of the first portion of condensate, in equilibrium with the reservoir of atmospheric water vapor; $F = W/W_O$, is the rain-out factor characterizing the removal of moisture from the reservoir of atmospheric water vapor (see text for details).

Table 4. Calculated $\delta^{18}O$/Temperature and $\delta^{18}O$/Precipitation Coefficients, Based on Monthly Data for $\delta^{18}O$ of Rainfall, Surface Air Temperature and the Amount of Precipitation for the Stations in the Region.

Station Name	Location	Altitude, masl	LMWL Slope/ Intercept	$\delta^2H/\delta^{18}O$ r^2	$\delta^{18}O$ versus Precipitation Slope r^2	$\delta^{18}O$ versus Temperature Slope r^2
			South Pacific Domain			
Tarawa	172.92°E, 1.35°N	4	8 04 /11.66	0.98	-0.019 (0.86)	(0.02)
Truk	151.85°E, 7.47°N	2	7.07 / 5.06	0.94	-0.014 (0.58)	(0.03)
Yap	138.09°E, 9.49°N	0	6.83 / 3.37	0.92	-0.018 (0.61)	(0.09)
Taguac	144.83°E, 13.55°N	110	7.01 / 6.10	0.93	-0.019 (0.89)	-2.414 (0.36)
Manila	121 00°E, 14.52°N	14	6.68 / 0.91	0.88	-0 012 (0.70)	(0.13)
Singapore	103.90°E, 1.35°N	32	7 52 / 9 53	0.97	-0.018 (0.41)	(0.00)
Ko Samui	100.03°E, 9.28°N	7	7.18 / 6.89	0.97	-0.010 (0.49)	(0.00)
Ko Sichang	100.80°E, 13.17°N	0	7.62 / 7.61	0.98	-0.012 (0.50)	0.532 (0.32)
Bangkok	100.50°E, 13.73°N	2	7.59 / 6.35	0.97	-0.019 (0.86)	(0.02)
Haikou	110.21°E, 20.02°N	15	7.89 / 11.04	0.97	-0.023 (0.44)	-0.562 (0.75)
Luang -Prabang	102.13°E, 19.88°N	305	7 94 / 8.34	0.97	-0.027 (0.55)	(0.13)
Kunming	102.68°E, 23.02°N	1841	7.48 / 5.81	0.95	-0.041 (0 65)	(0.24)
Lhasa	91.08°E, 29.42°N	3649	8.09 / 12.45	0.98	(0.14)	(0.00)
Hong-Kong	114.17°E, 22.32°N	65	8.04 / 10.56	0.96	-0.013 (0.76)	-0.399 (0.89)
Guangzhou	113.32°E, 23.13°N	7	7.76 / 5.37	0.83	-0.013 (0.35)	-0.377 (0.70)
Nanjing	118.18°E, 32.18°N	26	8.49 / 17.71	0.97	-0.015 (0.28)	(0.08)
Fuzhou	119 17°E, 26.05°N	16	8.19 / 11.73	0.92	(0.04)	(0.22)
Changsha	113.04°E, 28.12°N	37	8.41 / 15.05	0.97	(0.04)	-0.182 (0.46)
Guilin	110.08°E, 25.07°N	170	8.38 / 16.75	0.98	(0.03)	-0.299 (0.74)
Guiyang	106.43°E, 26.35°N	1071	8.82 / 22.06	0.98	-0.037 (0.38)	-0.287 (0.50)
Liuzhou	109.40°E, 24.35°N	97	7.19 / 1.41	0.91	(0.08)	-0.287 (0.65)
Wuhan	114.13°E, 30 62°N	23	8.70 / 14.26	0.94	(0.04)	(0.13)
Zunyi	106.88°E, 27.70°N	844	7.76 / 9.82	0.93	-0.043 (0.56)	-0.354 (0.67)
Chengdu	104 02°E, 30.67°N	506	7 64 / 3.50	0.94	-0.031 (0.56)	-0.371 (0.50)
Changqing*	106.60°E, 29.62°N	192	6.87 / 1.95	0.99	----------	----------
			North Pacific Domain			
Weathership V	164.00° E, 31.00°N	0	5.51 / -1.10	0.74	(0.02)	(0.22)
Wake Isl.	166.65° E, 19.28°N	3	6.85 / 6.13	0.82	-0.021 (0.81)	-0.622 (0.76)
Ryori	141 50° E, 39 02°N	260	7.68 / 11.03	0.92	0.012 (0.33)	0.092 (0.46)
Tokyo	139 77 °E, 35.68°N	4	6.87 / 4.70	0.84	0.011 (0.28)	0.082 (0.41)
Jinzhou*	121.10° E, 41.13°N	66	5.75 / -11.40	0.80	(0.12)	(0.00)
Pohang	129.38° E, 36.03°N	6	8.08 / 12 92	0.86	-0.012 (0.61)	-0.097 (0.76)
Yantai	121.40° E, 37.53°N	47	6.29 / -3.63	0.81	----------	----------
Tianjin	117.10° E, 39.06°N	3	7.45 / 6.60	0.95	(0.04)	0.152 (0.30)
Shijiazuang	114.25° E, 38.02°N	80	6.70 / -1.76	0 88	(0.06)	0.130 (0.35)
Taiyuan	112.55° E, 37.78°N	778	6.42 / -4.66	0.95	----------	--------
Zhengzhou	113.65° E, 34.72°N	110	6.75 / -2.71	0.88	(0.01)	(0.00)
Xian	108.93° E, 34.30°N	397	7.49 / 6.13	0.92	(0.09)	(0.17)
Haerbin	126 62° E, 45.68°N	172	5.97 /-14.34	0.86	----------	----------
			Indian Ocean Domain			
Colombo*	79.52° E, 6.54° N	5	7.93 / 9.68	0.96	----------	----------
Salagiri*	79.44° E, 6.54° N	550	7.05 / 2 59	0.99	----------	----------
Bombay	72.82° E, 18.90° N	10	7.94 / 8.39	0.94	(0.21)	(0.08)
Karachi	67.13° E, 24.90° N	23	7.60 / 3.69	0 93	----------	----------
New Delhi	77.20° E, 28.58° N	212	7.11 / 3.97	0 95	-0.020 (0.27)	(0.03)
Allahabad*	81 44° E, 25.27° N	98	7.56 / 4.61	1.00	----------	----------
Shillong	91.88° E, 25.57° N	1598	8.02 / 11.88	0.98	(0.19)	-0.652 (0.40)
Yangoon	96.17° E, 16 77° N	20	7.48 / 3.80	0.96	(0 06)	(0.02)

Table 4 (continued)

Station Name	Location	Altitude, masl	LMWL Slope/ Intercept	$\delta^2H/\delta^{18}O$ r^2	$\delta^{18}O$ versus Precipitation Slope r^2	$\delta^{18}O$ versus Temperature Slope r^2
			Central Asia Domain			
Kabul	69.08° E, 34.67° N	1860	7.33 / 12.37	0 97	(0.23)	0.400 (0.87)
Tashkent*	69.27° E, 41.27° N	428	9 43 / 21.95	0.86	----------	----------
Omsk*	73.24° E, 54.56° N	94	7.51 / 0.52	0 97	----------	----------
Hetian	79.56° E, 37.08° N	1375	8 40 / 11.46	0.99	0.278 (0.46)	0.718 (0.93)
Wulumiqi	87.62° E, 43.78° N	918	7.21 / 2 61	0.97	0.496 (0.67)	0.435 (0.94)
Zhangye	100.43° E, 38.93° N	1483	7 38 / 3.19	0 97	0.476 (0.59)	0.555 (0.94)
Novosibirk*	82.90° E, 55.03° N	162	8.77 / 24 10	0.97	0.191 (0.45)	0.321 (0.77)
Enisejsk*	92.09° E, 58 27° N	98	8 68 / 6.53	0.99	(0.22)	0 305 (0.68)
			Arctic Domain			
Irkutsk	104.35° E, 52.27° N	485	8 05 / 6.78	0.97	0 107 (0.49)	0.391 (0.83)
Ulan Bator*	106.59° E, 47.56° N	1338	7 93 / -3.31	0.99	----------	----------
Baotou	109 85° E, 40.67° N	1067	6.36 / -5 21	0.93	(0.22)	0.227 (0 66)
Yinchuan	106.13° E, 38.29°N	1112	7.27 / 5.76	0.96	0.221 (0.51)	0 409 (0.74)
Lanzhou	103.88° E, 36.05° N	1517	7.15 / 5.83	0.97	0.119 (0.55)	0.349 (0.42)
Qiqihar	123.55° E, 47.23° N	147	7 58 / -0 17	0.98	0.083 (0 47)	0.422 (0.89)
Habarovsk*	135.17° E, 48.52° N	72	7.85 / 5.93	0.97	0.076 (0.48)	0.212 (0.43)

The slope and the intercept of the Local Meteoric Water Line (LMWL) for each analyzed station, based on monthly $\delta^{18}O$ and δ^2H data, are included.

of the local rainfall. In the following discussion the stations in the region will be combined into groups (domains) exhibiting similar seasonal variability of isotope and meteorological data.

5.1. South Pacific Domain

This region is represented by three stations located on small islands in the equatorial Pacific (Tarawa, Truk, and Yap) and three coastal stations (Manila, Singapore, and Bangkok). Station Taguac (Guam Island), although located at 13.5°N latitude, also belongs to this group owing to similar seasonal behavior of isotope and meteorological parameters (Figure 6).

The island stations mentioned above can be considered representative of the source region of the Pacific monsoon. They are characterized by high annual precipitation (between 2,390 mm for Tarawa and 3,580 mm and for Truk) and small seasonal variability of temperature. The seasonal distribution of rainfall reveals a broad maximum during summer (April-October), with the exception of Tarawa, which has higher rainfall in the winter months (November-January).

The seasonal variability of $\delta^{18}O$ in this region is controlled by the amount effect [*Lawrence and White*, 1991; *Rozanski et al*, 1993]. There is a strong inverse relationship between the mean monthly $\delta^{18}O$ and the amount of precipitation, whereas the correlation with the mean monthly surface air temperature is virtually nonexistent (Table 4). The seasonal changes of $\delta^{18}O$ are very similar at all stations, with a broad minimum during the summer months corresponding to enhanced precipitation. Low $\delta^{18}O$ values during November, December, and January at Tarawa are consistent with higher rainfall recorded during this time period at this station. The deuterium-excess values fluctuate around the value of $+10^0/_{00}$, without any visible seasonal trend.

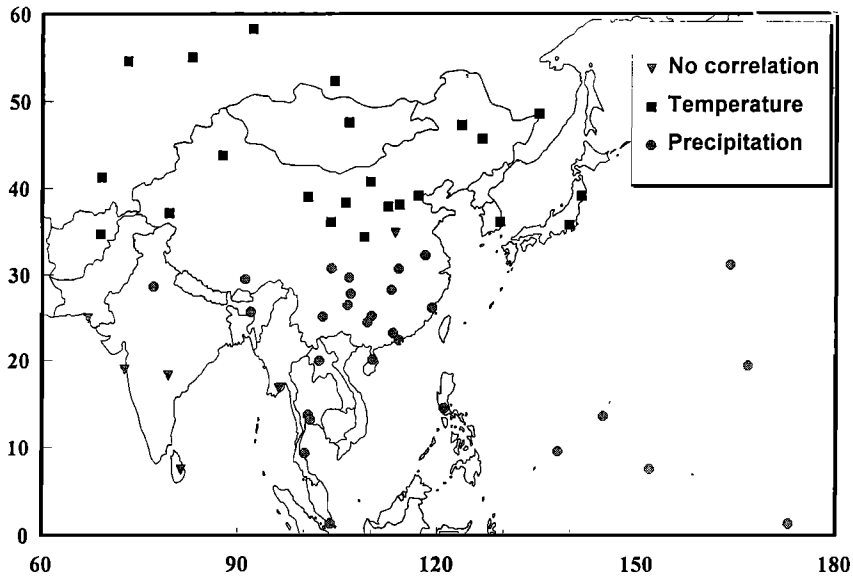

Figure 5. Areas of different response of isotopic composition of precipitation in the region to changes of surface air temperature and the amount of precipitation, based on the long-term monthly means of isotope and meteorological data.

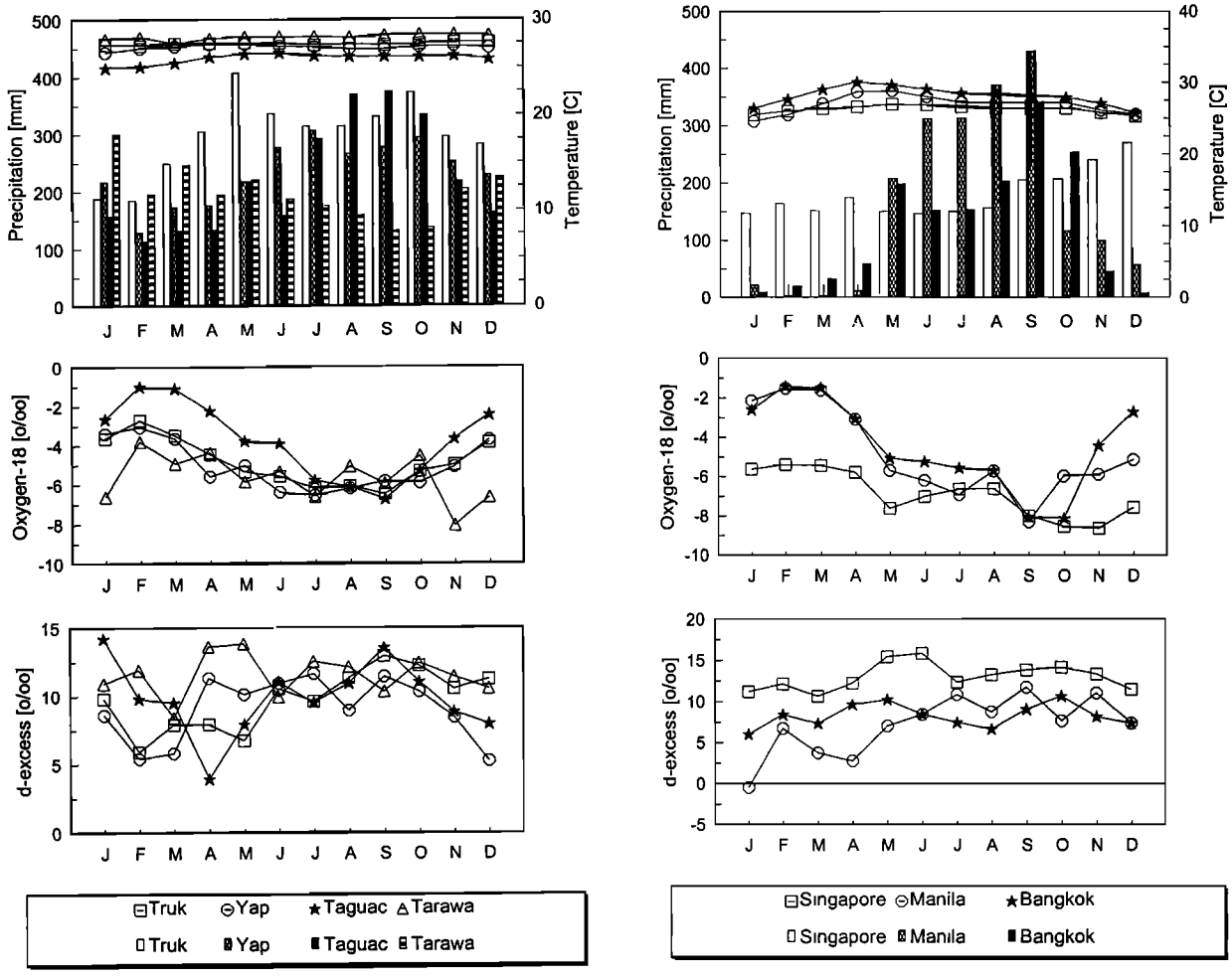

Figure 6. Seasonal variability of meteorological (mean monthly surface air temperature and the amount of rainfall) and isotope ($\delta^{18}O$ of monthly rainfall and the corresponding deuterium excess) data for the stations on islands located in the (left) western equatorial Pacific and (right) Far East.

The relatively low $\delta^{18}O$ values of rainfall in this region, when compared with the adjacent oceanic sites (e.g., Wake Island), have been noted in earlier surveys [*Dansgaard*, 1964; *Gonfiantini*, 1985]. This can be qualitatively explained as the combined effect of the extent of rain-out process of deep convective clouds, being the major contributors to rainfall in this region, high precipitation intensity, recirculation of moisture, and isotope exchange processes beneath the cloud base [*Yapp*, 1982; *Rozanski et al.*, 1993; Gedzelman and Arnold, 1994).

The stations located to the west and northwest, in the general direction of the Pacific monsoon (Manila, -6.7‰; Bangkok, -6.6‰), reveal slightly lower annual weighted mean $\delta^{18}O$ values of rainfall when compared with the sites located in the source area. The ground level temperature at these sites does not change significantly with the season. Precipitation at Manila and Bangkok shows a distinct maximum during summer, associated with the monsoon activity (Figure 6). Seasonal changes of $\delta^{18}O$ are controlled by the amount effect, showing a broad minimum in summer and early autumn. Although the Singapore station, being located outside the main track of the Pacific monsoon, reveals very similar isotopic depletion of rainfall as Manila and Bangkok ($\delta^{18}O$=-6.9‰), it does not show a typical, monsoon-controlled division into dry and rainy periods. It receives between 150 and 250 mm per month, with apparent small maximum toward the end of the year. Consistently higher deuterium-excess values are recorded at this station (between 10 and 15‰) pointing to a different source of rainfall.

Southeast China is represented by two coastal stations (Hong Kong and Haikou) and three stations located farther inland (Changsha, Wuhan, and Zhengzhou), in the general direction of the Pacific monsoon track (Figure 7). The inland stations experience in March-April elevated $\delta^{18}O$ values (around -2.5‰), also visible in Nanjing (not shown in Figure 7), combined with relatively high deuterium excess values. This indicates proximity of moisture source, most probably the Yellow Sea. The arrival of monsoon at these stations, is marked by the increase of rainfall and the corresponding drop of its $\delta^{18}O$ value. This drop is spectacular at the inland stations: more that 5‰ from May to June. The second rainy period in September-October may be associated with the southward movement of the ITCZ.

5.2. Indian Ocean Domain

The region controlled by the Indian monsoon is represented by two coastal stations (Bombay and Yangoon) and one station located in the center of the Indian continent (New Delhi); see Figure 8. The monsoon rains first set in at Yangoon (May), followed by Bombay (June). At New Delhi the maximum of rainfall occurs during July and August. The highest precipitation rate is observed in Bombay during June and July. The isotope

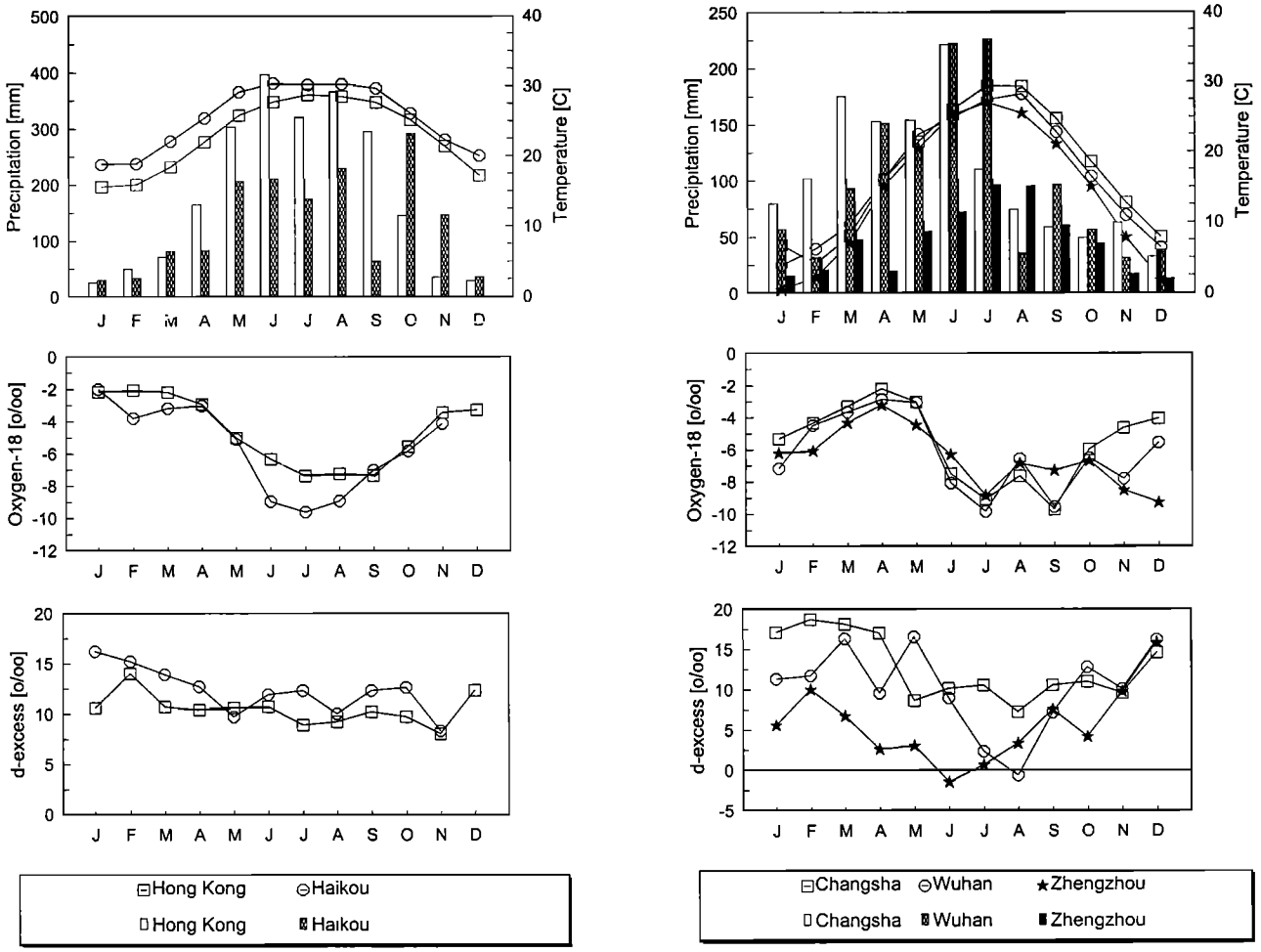

Figure 7. Seasonal variability of meteorological (mean monthly surface air temperature and the amount of rainfall) and isotope ($\delta^{18}O$ of monthly rainfall and the corresponding deuterium excess) data for the coastal stations of (left) south China and (right) continental stations located along the track of the Pacific monsoon.

data reveal several interesting features. At Yangoon the $\delta^{18}O$ starts to decrease only in August, 2 months after the monsoon actually sets in. It continues to drop, reaching the minimum in October (southward passage of ITCZ) when the rainfall is already significantly smaller than during the peak of monsoon. This effect is even more pronounced at Bombay which experiences heavy rainfall during June, July and August (between 400 and 700 mm per month) while $\delta^{18}O$ remains relatively high (around $-1^{0}/_{00}$) pointing to a local source of moisture (probably the Arabian Sea). The $\delta^{18}O$ remains high even in September, when rainfall declines to less than half of the maximum observed in July, and then drops to $-4.5^{0}/_{00}$ in October and $-5.4^{0}/_{00}$ in November, when only traces of rain are usually observed. This depletion is most probably due to a reversing of circulation from southeast to northwest and the southward passage of the ITCZ. It should be noted that low $\delta^{18}O$ values in October-November are observed in a number of other stations in the region; namely Yangoon, Singapore, Bangkok, and others.

The isotopic composition of rainfall at New Delhi was discussed by *Datta et al.* [1991]. The dry period (less than 25 mm per month) occurs from January to May, with $\delta^{18}O$ values of rainfall between +1 and -1 per mil. These high $\delta^{18}O$ values point to local, recycled moisture (evaporation of nearby surface water bodies, evaporation of soil moisture) as a major source of rainfall during these months. However, partial evaporation of raindrops on the way to the rain gauge might also be an important factor leading to relatively enriched $\delta^{18}O$ values. Gradually decreasing d-excess values of rainfall at New Delhi during this period, associated with raising air temperatures, suggest that the observed increase of $\delta^{18}O$ from $-1.5^{0}/_{00}$ in January to $+1^{0}/_{00}$ in May might, in fact, be caused by enhanced evaporation of raindrops below the cloud base. The monsoon rains arrive from the Bay of Bengal, already partially depleted in heavy isotopes owing to the rain-out effect on the way to New Delhi [*Krishnamurthy and Bhattacharya*, 1991]. The $\delta^{18}O$ reaches the minimum of about $-8.6^{0}/_{00}$ in September and returns to $-1.5^{0}/_{00}$ in December.

5.3 North Pacific Domain

This source region is represented by two oceanic sites: Wake Island and Weathership V (Figure 9). Wake Island is situated in a typical transition zone between the humid, warm climate of the equatorial Pacific and a moderate maritime climate with well-developed seasonality in temperature and rainfall evenly distributed throughout the year. In general, the mean annual $\delta^{18}O$ is significantly higher than in the equatorial Pacific ($-2.1^{0}/_{00}$ for Wake Island and $-4.3^{0}/_{00}$ for Weathership V). The seasonal changes of $\delta^{18}O$ at Wake Island are controlled mainly by the amount effect. At Weathership V a slight minimum of $\delta^{18}O$

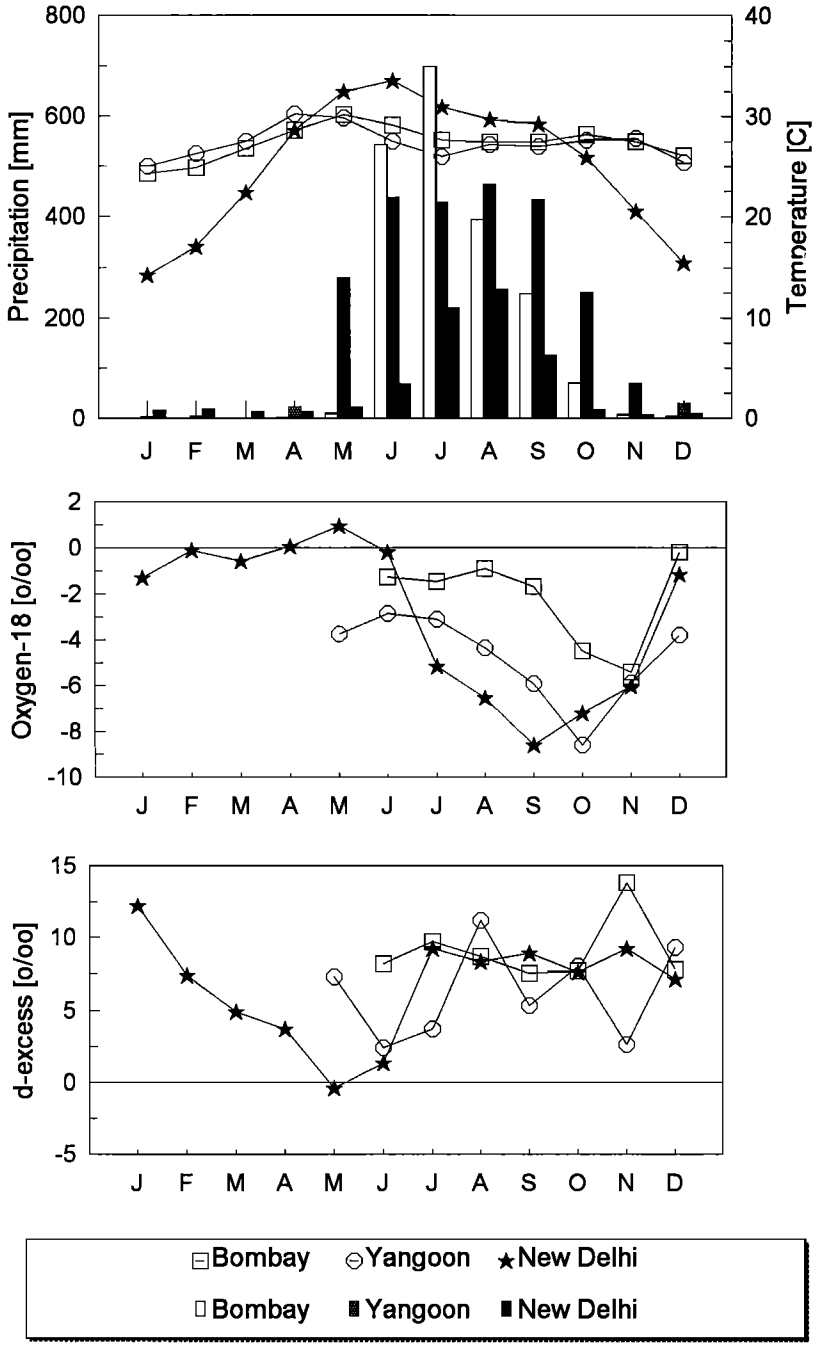

Figure 8. Seasonal variability of meteorological (mean monthly surface air temperature and the amount of rainfall) and isotope ($\delta^{18}O$ of monthly rainfall and the corresponding deuterium excess) data for the stations representing the Indian monsoon domain.

during the summer months (June-September) is observed, accompanied by an increase in temperature. There is a tendency toward higher *d*-excess values during the winter months in this region, clearly visible at the Weathership V site. A likely reason for this is the substantially cooler surface of the North Pacific during winter (about 13°C) as compared to about 22°C during summer (the region between 20°N and 40°N).

The coastal stations, Tokyo, Ryori and Pohang reveal distinct seasonality in both temperature and the amount of rainfall, with the maximum during summer. There is little seasonal variability of $\delta^{18}O$, but a well-marked seasonal trend in deuterium excess, with high *d* values during winter (15-25‰) and low values during summer (5-10‰). This seasonality of the *d*-excess stems mainly from a complete reversal of the circulation patterns. During the winter months, dry air masses from the northern Asian continent pass the Sea of Japan and the Yellow Sea, picking up moisture under reduced relative humidity and lower sea surface temperature. This leads to relatively high $\delta^{18}O$ values of winter rainfall (proximity of the source of moisture) and high d-excess values. In summer the stations receive precipitation predominantly from the Pacific Ocean, with relatively low $\delta^{18}O$ values (compare with $\delta^{18}O$ values recorded at Weathership V during summer) and low *d*-excess values. High *d*-excess signatures of rainfall due to the interaction of relatively dry air

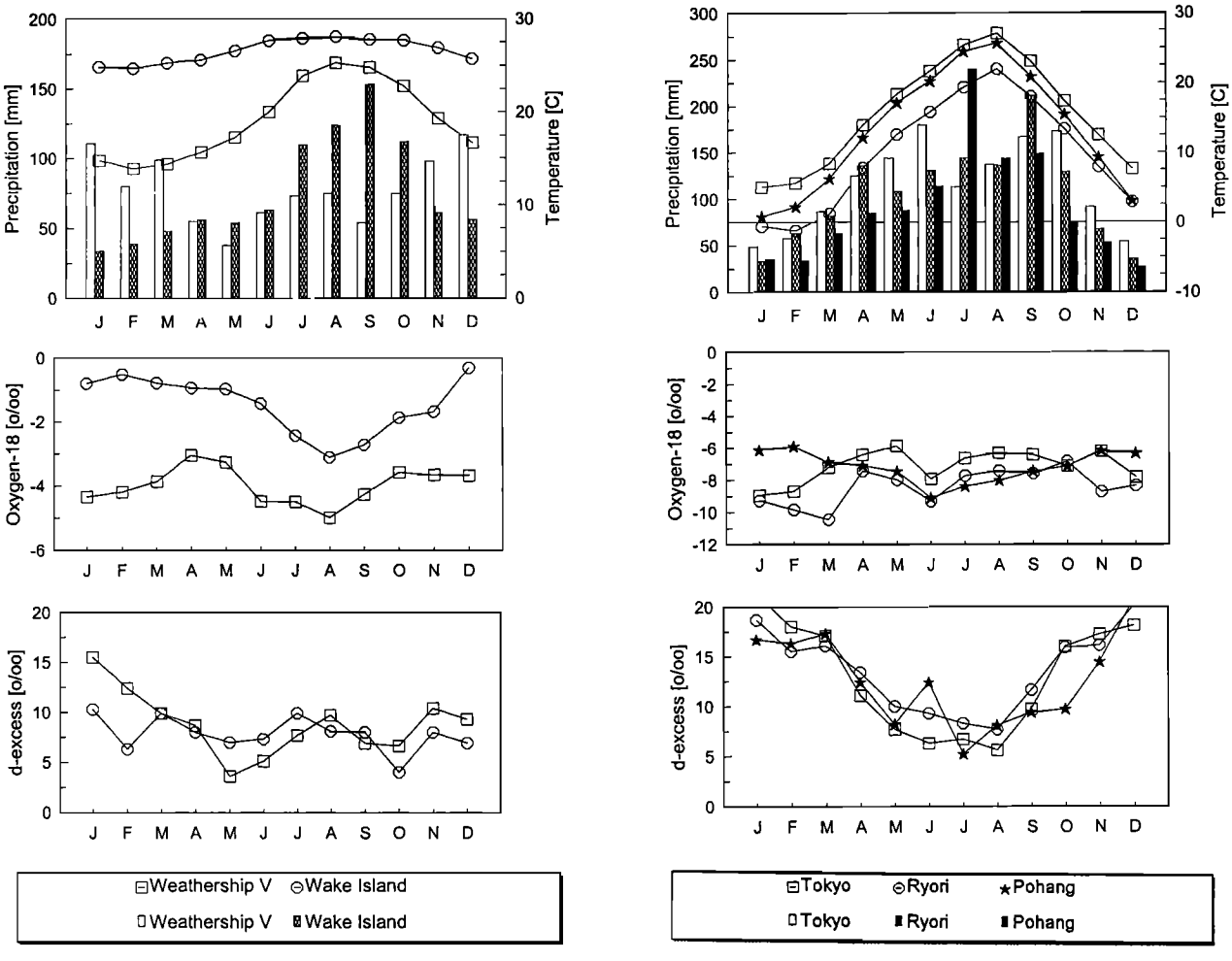

Figure 9. Seasonal variability of meteorological (mean monthly surface air temperature and the amount of rainfall) and isotope ($\delta^{18}O$ of monthly rainfall and the corresponding deuterium excess) data for the stations located in the (left) North Pacific and (right) coastal stations of Japan and the Korean Peninsula.

masses with large surface water bodies have been observed in the eastern Mediterranean region [*Gat and Carmi,* 1987].

The stations located farther inland (Tianjin and Shijiazuang) reveal a more pronounced seasonal variability of temperature and rainfall, when compared with the coastal stations (Figure 10). In July and August the Pacific monsoon arrives at this latitude, producing a distinct maximum of rainfall, which is depleted in heavy isotopes. The much more pronounced minimum of $\delta^{18}O$ is observed during the winter months (December-February), associated with relatively high values of deuterium excess. These elevated values of *d*-excess indicate the presence of continental air masses producing precipitation during the winter months (see 5.4 and 5.5).

The next group of stations (Baotou, Yinchuan, Zhangye, and Lanzhou; see Figure 10) represents temperate, dry continental climate of the boundary region between northwest China and Inner Mongolia [*Winkler and Wang*, 1993]. This region is beyond the reach of the Pacific monsoon and receives continental air masses from the north and northwest during winter. Only at Yinchuan can a slight decrease of $\delta^{18}O$ in July be seen, suggesting contribution of monsoon rains. The $\delta^{18}O$ varies in accordance with changes of temperature, from approximately $-20^{0}/_{00}$ in December and January to around $-2^{0}/_{00}$ in July at Zhangye station.

5.4. Arctic Domain

This region is represented by Irkutsk (Russian Federation) and two stations located in northeast China (Haerbin and Qiqihar); see Figure 11. All three stations experience typical continental climate with mean surface air temperatures of around -15°C and $\delta^{18}O$ values of $-25^{0}/_{00}$ during the winter months. During summer, temperatures reach 20°-25°C and $\delta^{18}O$ oscillates around $-10^{0}/_{00}$ Deuterium excess is generally low, between 0 and $10^{0}/_{00}$.

5.5 Central Asia Domain

The central Asian region is represented by two stations located in northwestern China (Wulumiqi and Hetian) and by Kabul station (Afghanistan). Although all three sites reveal similar seasonality in temperature, with marked differences during winter months, seasonal distribution of rainfall at Kabul is in antiphase with the two Chinese stations; the rainy period in Kabul occurs during the winter months (Figure 11), indicating that different air masses are producing precipitation within this domain. A different origin of moisture-producing winter precipitation at Kabul, when compared with Wulumiqi and Hetian, seems to be confirmed also by large differences in the $\delta^{18}O$ values during winter (October-April); around $-15^{0}/_{00}$ for Wulumiqi and Hetian

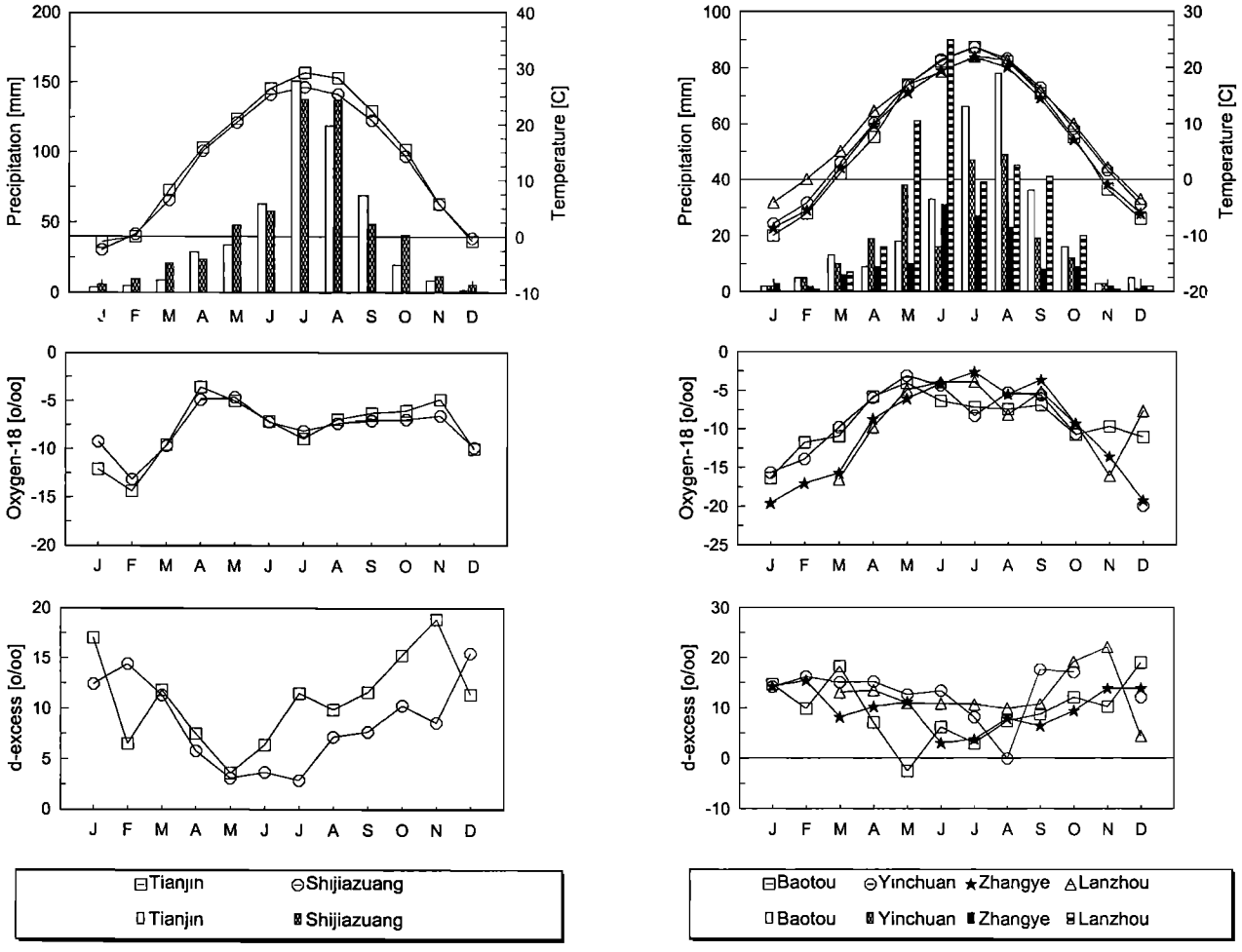

Figure 10. Seasonal variability of meteorological (mean monthly surface air temperature and the amount of rainfall) and isotope ($\delta^{18}O$ of monthly rainfall and the corresponding deuterium excess) data for the stations located in the (left) coastal region of northern China and (right) boundary region between northwest China and Inner Mongolia.

and only around $-8^0/_{00}$ for Kabul. The difference in the mean air temperatures for this period reaches only approximately 5°C. The $\delta^{18}O$ values close to $0^0/_{00}$ during summer months at Kabul, associated with relatively low *d*-excess values, might be indicative of partial evaporation of raindrops below the cloud base. However, this explanation does not hold for Hetian, showing relatively high *d*-excess values in summer. In case of Hetian a contribution of recycled moisture derived from local sources could be a likely reason for elevated $\delta^{18}O$ values (see discussion in Section 6).

The complexity of the seasonal variations of the isotopic composition of precipitation in southeast Asia is illustrated by Figures 12 and 13, in which the long-term monthly means of $\delta^{18}O$ are plotted as a function of temperature, precipitation amount, and water content of the near-ground atmosphere. The data points are labeled by corresponding months. The dashed lines represent best linear fits of all individual monthly values. Figure 12 compares the seasonality in the above-mentioned parameters, typical for the western Pacific region (Wake Island), with those observed in a extremely continental environment (station Wulumiqi in the northwest corner of China). Figure 13 presents an analogous comparison for Hong Kong and Lhasa stations. It is apparent from Figures 12 and 13 that the response of $\delta^{18}O$ of precipitation to seasonally changing meteorological parameters in the region can be very complex; the correlation with these parameters can be positive, negative, or completely missing. For some stations (e.g., Hong Kong and Lhasa) a distinct hysteresis effect is visible; that is, the same value of meteorological parameters occurring in different seasons corresponds to very different $\delta^{18}O$ values of rainfall. This is demonstrated by the data available for Lhasa station, where for the similar mean monthly temperature of April and October, the $\delta^{18}O$ values differ by as much as $15^0/_{00}$. This is a consequence of a different origin of the moisture-producing rainfall at Lhasa during these 2 months. During winter and spring the atmospheric moisture on the Tibetan Plateau is predominantly of local origin. High $\delta^{18}O$ values suggest a significant contribution of recycled moisture. During summer, very low $\delta^{18}O$ values are due to the rain-out effect of moist monsoon air masses.

6. Continentality

It is known that the distribution of $\delta^{18}O$ in precipitation mirrors the topography of continents. Mountainous regions are marked by more negative $\delta^{18}O$ values than the low-altitude regions. This feature is called "altitude effect." The apparent tendency to observe more negative $\delta^{18}O$ values of precipitation with increasing distance from the coast is known as "continental effect." Basically, the same mechanism is responsible for both

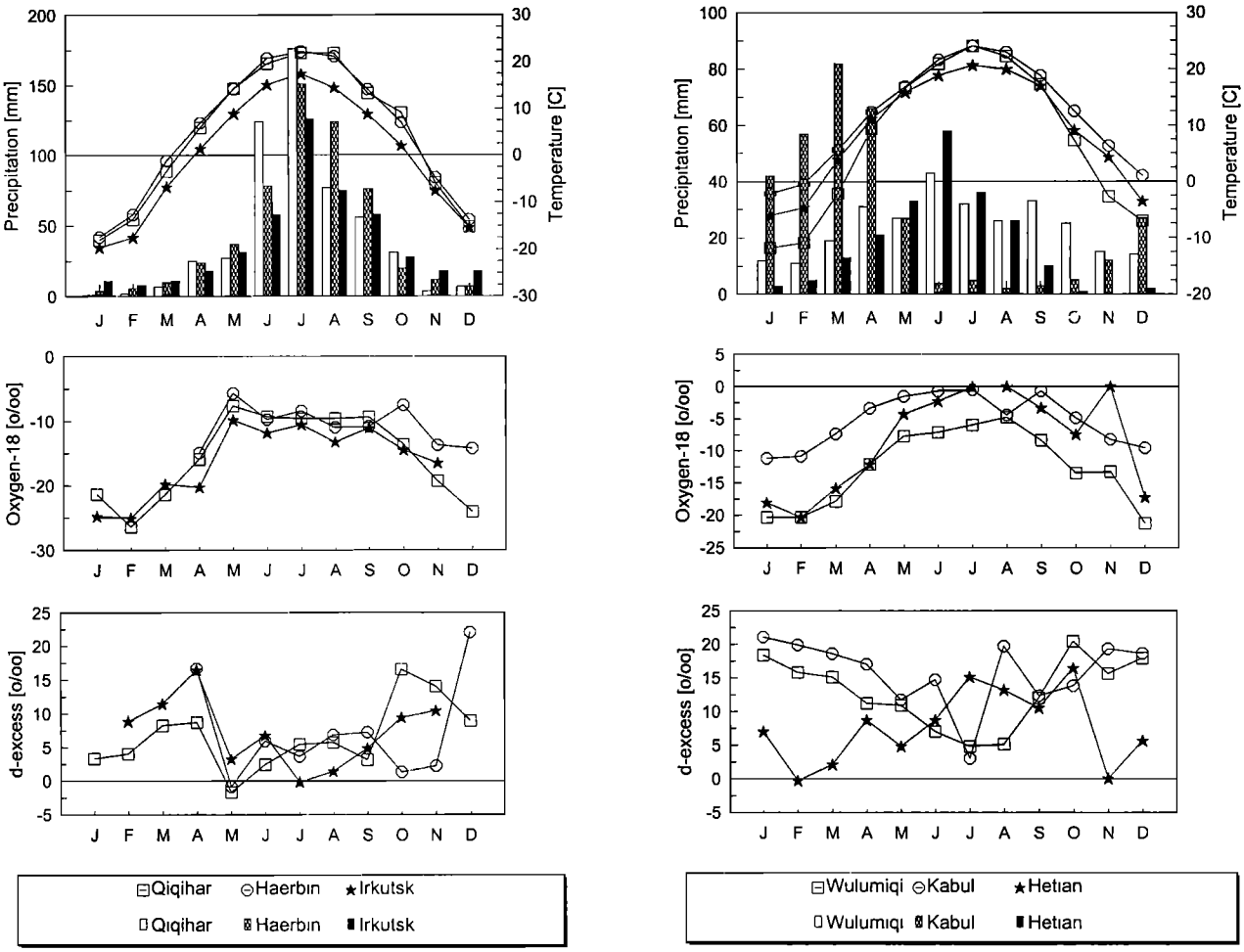

Figure 11. Seasonal variability of meteorological (mean monthly surface air temperature and the amount of rainfall) and isotope ($\delta^{18}O$ of monthly rainfall and the corresponding deuterium excess) data for the stations (left) remaining under the influence of continental air masses of Arctic origin and (right) located in the inner portion of the Asian continent.

effects, namely, the preferential removal of the heavy isotopes during the gradual removal of moisture from the air masses moving inland or being uplifted by orographic features, coupled with isotope effects during the condensation process. This implies that the atmospheric water vapor originates from a single source (specific region of the ocean). Such an assumption might, however, not always be fulfilled, e.g., in the vicinity of large continental water bodies or in the interior of continents where reevaporated moisture plays an important role in the atmospheric water balance [*Salati et al.*, 1979; *Sonntag et al.*, 1983; *Ingraham and Craig*, 1993].

Figure 14 shows two transects across the mainland of China: (1) latitudinal transect across the northern part of the discussed region, from Tokyo to Wullumiqi, and (2) longitudinal transect, along the general direction of the Pacific monsoon from Hong Kong to Zhangye. The weighted mean $\delta^{18}O$ values, calculated separately for the dry and the rainy periods, are plotted versus distance from the coast. For the northern transect the mean seasonal $\delta^{18}O$ values remain similar and roughly constant up to approximately 2000 km from Tokyo (stations Tianjin and Shijiazuang). Farther inland, with increasing elevation, the $\delta^{18}O$ curves diverge. During the winter months the $\delta^{18}O$ values decrease with increasing distance, whereas during summer, $\delta^{18}O$ increases farther inland up to Yinchuan and Zhangye station. The second transect clearly shows the influence of the monsoon. Up to about 700 km from Hong Kong (stations Guiyan and Changsha), the summer values of $\delta^{18}O$ are about $4^{0}/_{00}$ lower than the winter values. In both cases there is a slight decrease of $\delta^{18}O$ with distance. Farther inland, winter $\delta^{18}O$ values gradually decrease with increasing distance since the temperature becomes the main controlling parameter. The summer $\delta^{18}O$ values gradually increase in this part of the transect, indicating gradual weakening of the monsoon influence.

The spatial distribution of $\delta^{18}O$ in the studied region reveals an interesting feature: the summer mean $\delta^{18}O$ values (see Figure 2) show a "heavy spot" centered in north central China (stations Zhangye, Lanzhou, Yinchuan, and Baotou), despite the relatively high elevation of this region, between 1,000 and 1,500 masl. Anomalously heavy $\delta^{18}O$ values during summer are also observed at Hetian station, located in the southwest corner of China (1,375 masl; $-1.9^{0}/_{00}$). The reasons for this anomaly remain unclear.

On one hand, one may argue that these elevated $\delta^{18}O$ values are due to partial evaporation of rainfall either on the way from the cloud to the ground or in the rain gauge, under conditions typical for the semiarid climate of this region. Relatively low deuterium excess values at Zhangye, Lanzhou, Yinchuan, and Baotou, during summer (see Table 2) seem to confirm this

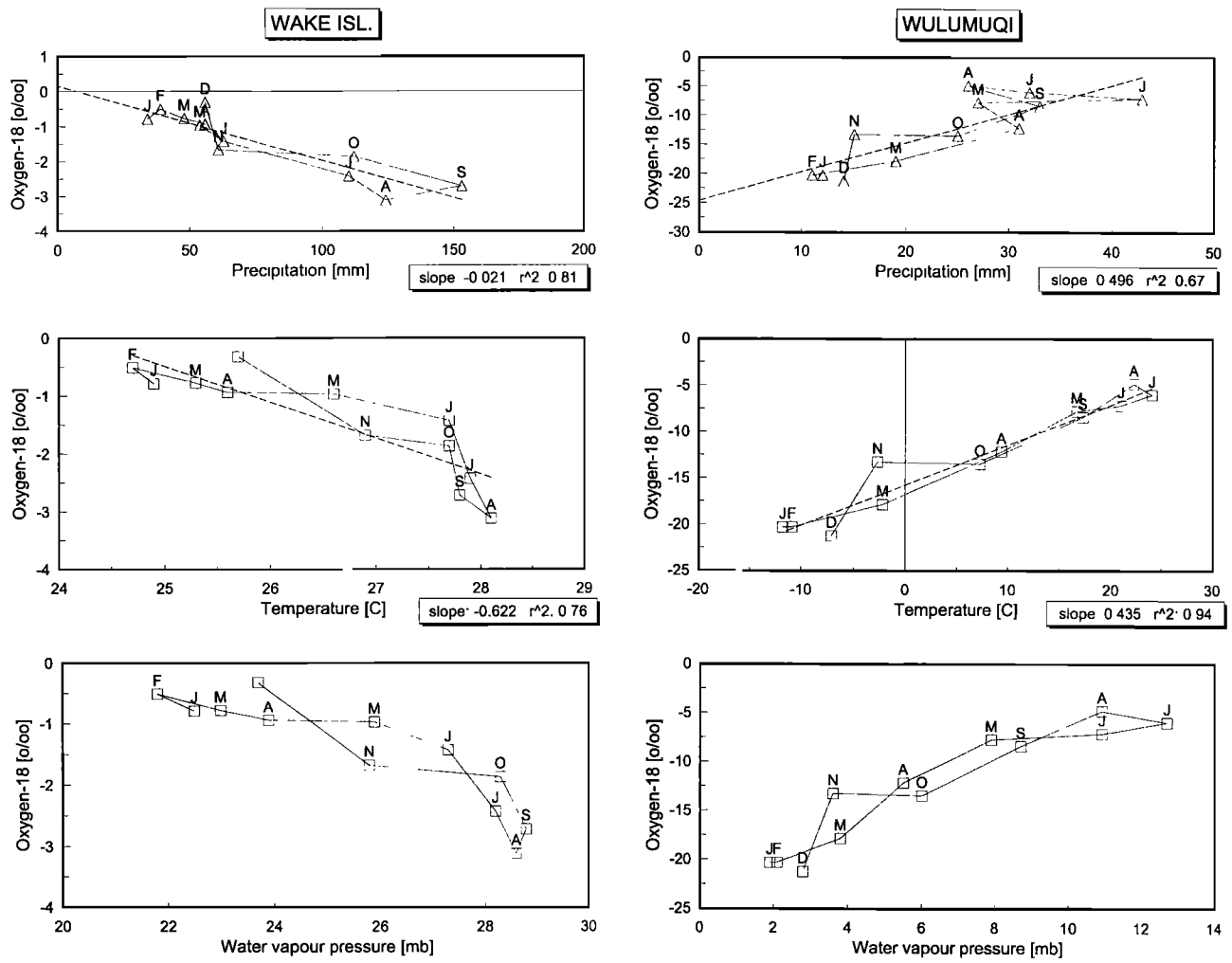

Figure 12. Long-term monthly means of $\delta^{18}O$ for (left) Wake Island (western Pacific) and (right) Wulumuqi (northeast China) plotted as a function of the amount of rainfall, surface air temperature, and water vapor pressure recorded at ground level. Letters indicate subsequent months. Best linear fits of the monthly data points are indicated by dashed lines.

hypothesis. The reduction of the *d*-excess by approximately $5^0/_{00}$ due to partial evaporation of raindrops in unsaturated atmosphere, under typical conditions of temperature and relative humidity observed at these stations in summer, implies an increase of $\delta^{18}O$ of rainfall by $2.0\text{-}2.5^0/_{00}$. However, it should be noted that anomalous $\delta^{18}O$ values observed at Hetian in summer cannot be explained in this way; deuterium excess at this station is substantially higher in summer than in winter.

The elevated $\delta^{18}O$ values in summer may also result from significant contribution of reevaporated moisture to the local water balance. The stations in north central China are located close to the extensive desert area (Gobi Desert). Also, Hetian is located on the edge of another large desert (Takla Makan Desert). From numerous studies in the Sahara it is known that diffusive discharge of groundwater can occur through large areas of desert, in regional depressions [Aranyossy et al., 1992]. It is likely that such diffusive groundwater discharge through regional depressions may occur also in the Gobi and Takla Makan deserts. The groundwater in such areas is often highly enriched in heavy isotopes. For instance, a study in the Gurinai Grassland area, Inner Mongolia, surrounded by the Gobi Desert, revealed that groundwater in this region is enriched in ^{18}O by approximately $4^0/_{00}$ with respect to local meteoric water [*Geyh and Gu*, 1992]. Even higher enrichments were identified aquifers in desert areas of Northern Africa and Arabian Peninsula (IAEA - unpublished data, 1997). It has been demonstrated that during steady state evaporation through sand column and/or transpiration by plant cover, the released vapor should have the same isotopic composition as the source water (groundwater). Consequently, the vapor being introduced into the atmosphere during such processes is isotopically much heavier than "free" atmospheric moisture. The presence of such vapor was confirmed in several field studies [e.g., Bariac et al., 1990; Yakir and Wang, 1996]. Since the areas of diffusive discharge might be large, it is not unlikely that re-evaporated moisture may represent a significant component of the local water balance in summer for the discussed regions of northwest and southwest China and may lead to anomalous isotope enrichment of summer rainfall on these areas.

7. Concluding Remarks

From the global perspective, southeast Asia reveals the most complex patterns of spatial and temporal distribution of stable isotope composition of precipitation. The meteorology, pluviometric regime, and, consequently, the isotopic composition of rainfall in this region is being shaped by five air masses of different origin: (1) polar air mass from the Arctic, (2)

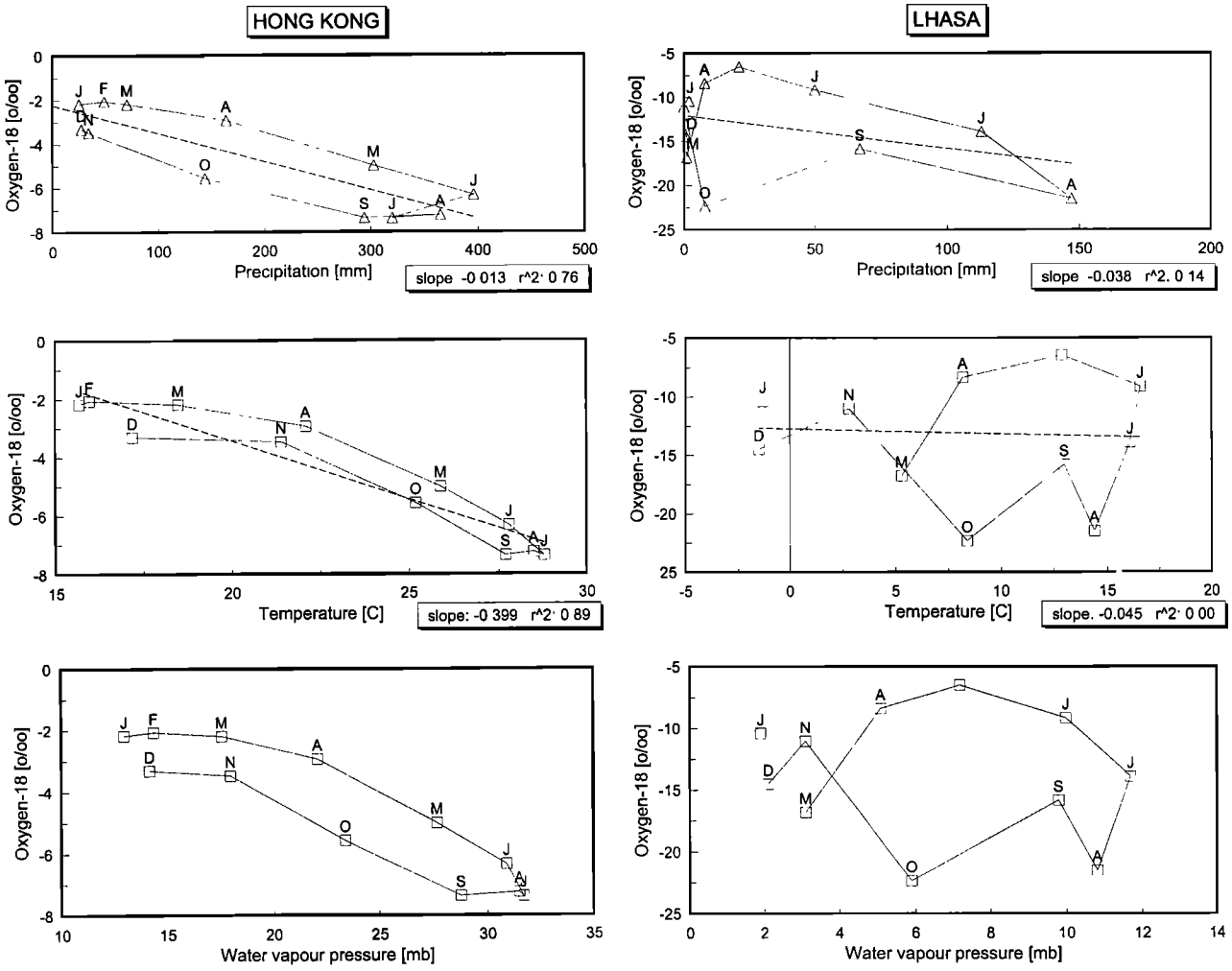

Figure 13. Long-term monthly means of $\delta^{18}O$ for (left) Hong Kong and (right) Lhasa (Tibetan Plateau), plotted as a function of the amount of rainfall, surface air temperature, and water vapor pressure recorded at ground level. Letters indicate subsequent months. Best linear fits of the monthly data points are indicated by dashed lines.

continental air mass coming from central Asia, (3) tropical-maritime air mass from the North Pacific, (4) equatorial-maritime air mass from the western equatorial Pacific, and (5) equatorial-maritime air mass from the Indian Ocean (Figure 1, bottom). The relative contribution of different air masses in the course of a year is modulated by the monsoon activity and the seasonal displacement of the Intertropical Convergence Zone (ITCZ).

Gradual rain-out of moist, oceanic air masses moving inland, associated with monsoon circulation, constitutes a powerful mechanism capable of producing large isotopic depletions in rainfall, even if there is no spatial/temporal change in the surface air temperature. This characteristic imprint of the monsoon activity is seen over large areas of southeast Asia. It is worth noting that the isotopic signatures of oceanic air masses forming two monsoon systems (Pacific and Indian monsoon) differ considerably: the average $\delta^{18}O$ of monsoon rainfall in the south of China is about $2.5^{0}/_{00}$ more negative than in the Bay of Bengal.

In addition to the data related to one of the isotopes (oxygen-18 or deuterium), the relation between both isotopes expressed by the deuterium excess can in some regions play an important role in identifying the origin of atmospheric moisture. High *d*-excess values in precipitation are indicative of low relative humidity in the oceanic source areas and/or the presence of secondary processes such as evaporation from open water bodies or partial evaporation of raindrops in unsaturated atmosphere below the cloud base. Strong seasonal variations of the deuterium excess observed in some areas of the studied region result most probably from a complete reversal of atmospheric circulation over these areas and changing source of atmospheric vapor (ocean versus continent). The isotope data available thus far seem to suggest that the moist air masses forming the Pacific and Indian monsoons differ not only with respect to their δ values but also in the markedly different deuterium excess values (around $5^{0}/_{00}$) between both systems. Thus isotopic composition of water vapor and rainfall can, in principle, be used to identify air masses belonging to these two monsoon systems.

This paper addresses only spatial and seasonal variability of isotopic composition of precipitation in the region. To date, only few stations (Hong Kong, Tokyo, Bangkok, and New Delhi) have sufficiently long and complete isotope records of $\delta^{18}O$ to justify analysis of the sensitivity of isotope signature of rainfall to long-term (decadal) changes of major indicators of climate. The isotope records available thus far for the stations located in mainland China are still too short to address quantitatively this question. On the other hand, the strong isotopic signal in precipitation associated with monsoon activity represents a powerful tool for reconstruction of changes in intensity and

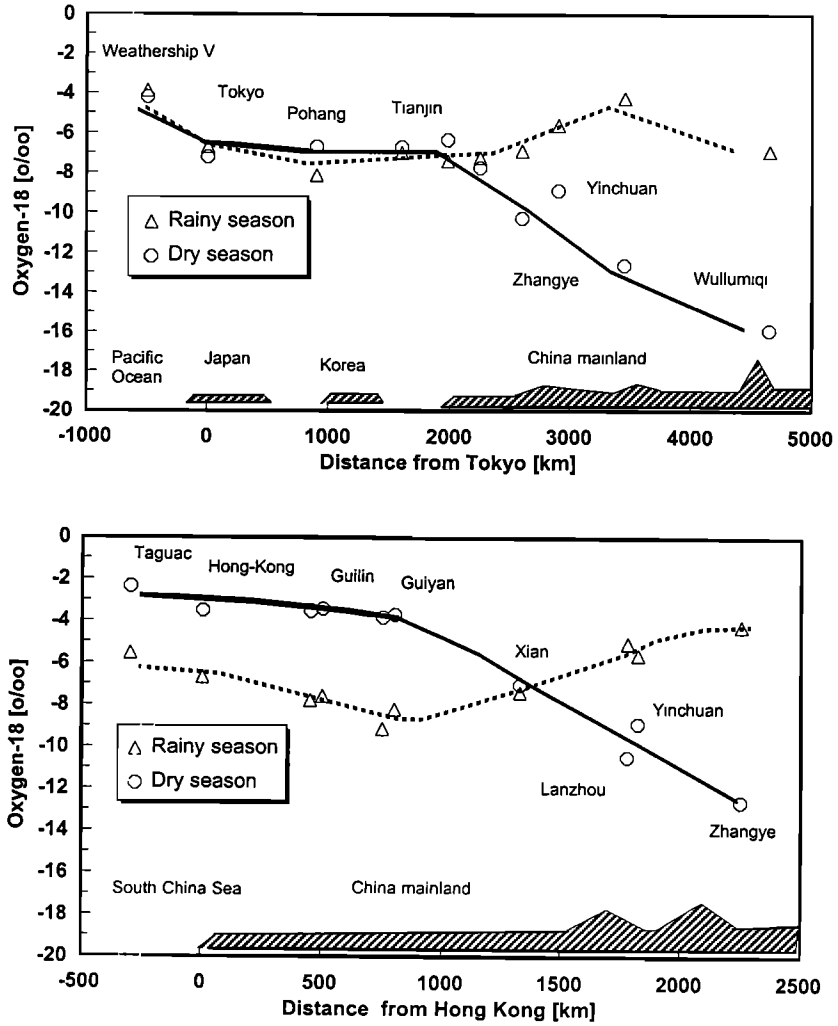

Figure 14. Changes of $\delta^{18}O$ of rainfall (weighted mean values for rainy and dry periods), along two transects: from (top) Tokyo to Wullumuqi and (bottom) Hong Kong to Zhangye.

extent of the Asian monsoon system in the past, especially close to the boundary regions. In fact, this tool has already been used to reconstruct changes in the intensity and extent of monsoon circulation during Holocene over the Tibetan Plateau, based on analyses of ^{18}O content of lacustrine carbonates [e.g., *Morinaga et al.*, 1993; *Gasse and van Campo*, 1994]. Also, attempts have been made to use isotopic composition of glacier ice to reconstruct past climatic and environmental changes in the region [e.g., *Thompson et al.*, 1989]. However, the potential for paleomonsoon studies of the isotopic signal imprinted in precipitation of the region still remains largely unexplored, mainly due to poor knowledge of the long-term sensitivity of isotopic composition of rainfall in the area. Therefore continuous efforts toward better characterization of the spatial and temporal variability of isotopic composition of precipitation in southeast Asia through expanded monitoring activities and the atmospheric general circulation model studies are essential for a better understanding of the key mechanisms controlling the climate of the region.

Acknowledgements. The continuous cooperation and support of numerous individuals and institutions in the region in maintaining the stations of the IAEA/WMO Global Network Isotopes in Precipitation are gratefully acknowledged. The isotope and meteorological data discussed in this paper are available through http://www.iaea.org/programs/ri/gnip/gnipmain.html

References

Aranyossy, J. F., A. Filly, A. A. Tandia, D. Louvat, B. Ousmane, A. Joseph, and J.-C. Fontes, Estimation des flux d'evaporation diffuse sous couvert sableux en climat hyper-aride (erg de Bilma, Niger), in *Isotope Techniques in Water Resources Development 1991*, pp. 309-324, Int. At. Energy Agency, Vienna, 1992.

Bariac, T., C. Jusserand, and A. Mariotti, Evolution spatio-temporelle de la composition isotopique de l'eau dans le continuum sol-plante-atmosphère, *Geochim. Cosmochim. Acta, 54*, 413-424, 1990.

Bryson, R.A., Airstream climatology of Asia, in *Proceedings of the International. Symposium on the Qinghai-Xizang Plateau and Mountain Meteorology*, pp. 604-617, Am. Meteorol. Soc., Boston, Mass., 1986.

Charles, C. D., D. Rind, J. Jouzel, R. D. Koster, and R.G. Fairbanks, Glacial-interglacial changes in moisture sources for Greenland: Influence on the ice core record of climate, *Science, 263*, 508-511, 1994.

Craig, H., Isotopic variation in meteoric waters, *Science, 133*, 1702-1703, 1961.

Craig, H., and L. Gordon, Deuterium and oxygen 18 variation in the ocean and marine atmosphere, in *Stable Isotopes in Oceanographic Studies and Palaeotemperatures, Spoleto 1965*, edited by E. Tongiorgi, pp. 9-130, Cons. Naz. delle Ric., Pisa, Italy, 1965.

Dansgaard, W., Stable isotopes in precipitation, *Tellus, 16*, 436-468, 1964.

Datta, P. S., S. K. Tyagi, and H. Chandrasekharan, Factors controlling stable isotope composition of rainfall in New Delhi, India, *J. Hydrol., 128*, 223-236, 1991.

Edwards, T. W. D., Interpreting past climates from stable isotopes in continental organic matter, in *Climate Change in Continental Isotopic Records, Geophys. Monogr. Ser.*, vol. 78. edited by P.R. Swart, et al., pp. 333-343, AGU, Washington D.C., 1993.

Fisher, D. A., Remarks on the deuterium excess in precipitation in cold regions, *Tellus, ser B, 43B*, 401-407, 1991.

Gasse, F., and E. van Campo, Abrupt, post-glacial climate events in West Asia and North Africa monsoon domains, *Earth Planet. Sci. Lett., 126*, 435-456, 1994.

Gat, J. R., and I. Carmi, Effect of climate changes on the precipitation patterns and isotopic composition of water in a climate transition zone: Case of the Eastern Mediterranean Sea area, in The Influence of Climatic Variability on the Hydrologic Regime and Water Resources, *IAHS Publ. 168*, 513-523, 1987.

Gedzelman, S. D., Deuterium in water vapour above the atmospheric boundary layer, *Tellus, Ser. B, 40B*, 134-147, 1988.

Gedzelman, S. D. and R. Arnold, Modelling the isotopic composition of precipitation, *J. Geophys. Res., 99*, 10,455-10,471, 1994.

Geyh, M. A., and W. Gu, Preliminary isotope hydrological study in the arid Gurinai grassland area, Inner Mongolia, in *Isotope Techniques in Water Resources Development 1991*, pp. 661-663, Int. At. Energy Agency, Vienna, 1992.

Gonfiantini, R., On the isotopic composition of precipitation in tropical stations, *Acta Amazonica, 15*, 121-139, 1985.

Ingraham, N. L., and R. C. Craig, Constraining estimates of evapotranspiration with hydrogen isotopes in a seasonal orographic model, in *Climate Change in Continental Isotopic Records, Geophys. Monogr. Ser.*, vol. 78. edited by P.R. Swart, et al.., pp.47-55, AGU, Washington D.C., 1993.

International Atomic Energy Agency, World survey of isotope concentrations in precipitation., *Tech. Rep. Ser.* vol. 69, Vienna, 1969.

International Atomic Energy Agency, World survey of isotope concentrations in precipitation., *Tech. Rep. Ser.* vol. 117, Vienna, 1970.

International Atomic Energy Agency, World survey of isotope concentrations in precipitation., *Tech. Rep. Ser.* vol. 129, Vienna, 1971.

International Atomic Energy Agency, World survey of isotope concentrations in precipitation., *Tech. Rep. Ser.* vol. 147, Vienna, 1973.

International Atomic Energy Agency, World survey of isotope concentrations in precipitation., *Tech. Rep. Ser.* vol. 165, Vienna, 1975.

International Atomic Energy Agency, World survey of isotope concentrations in precipitation., *Tech. Rep. Ser.* vol. 192, Vienna, 1979.

International Atomic Energy Agency, World survey of isotope concentrations in precipitation., *Tech. Rep. Ser.* vol. 226, Vienna, 1983.

International Atomic Energy Agency, World survey of isotope concentrations in precipitation., *Tech. Rep. Ser.* vol. 264, Vienna, 1986.

International Atomic Energy Agency, World survey of isotope concentrations in precipitation., *Tech. Rep. Ser.* vol. 311, Vienna, 1990.

International Atomic Energy Agency, Statistical treatment of data on environmental isotopes in precipitation, *Tech. Rep Ser.*, vol. .331, 720 pp., Vienna, 1992.

International Atomic Energy Agency, World survey of isotope concentrations in precipitation., *Tech. Rep. Ser.* vol. 371, Vienna, 1994.

Johnsen, S. J., W. Dansgaard, and J. W. C. White, The origin of Arctic precipitation under present and glacial conditions, *Tellus,Ser. B, 41B*, 452-468, 1989.

Joseph, A., J. P. Frangi, and J. F. Aranyossy, Isotope characteristics of meteoric water and groundwater in the Sahelo-Sudanese Zone, *J. Geophys. Res., 97*, 7543-7551, 1992.

Jouzel, J., and L. Merlivat, Deuterium and oxygen-18 in precipitation, modelling of isotopic effects during snow formation, *J. Geophys. Res., 89*, 11,749-11,757, 1984.

Krishnamurthy, R. V., and S. K. Bhattacharya, Stable oxygen and hydrogen isotope ratios in shallow groundwaters from India and a study of the role of evapotranspiration in the Indian monsoon, in Stable Isotope Geochemistry: A Tribute to Samuel Epstein, edited by H.P. Taylor, et al., *Spec. Publ R. Soc. Chem., 3*, 187-195, 1991.

Kuznetsova, L. P., Use of data on atmospheric moisture transport over continents and large river basins for the estimation of water balances and other purposes, Tech. Doc. Hydrol., IHP-III proj. 1.1, 105 pp., UNESCO, Paris, 1990.

Lawrence, J. R., and J. W. C. White, The elusive climate signal in the isotopic composition of precipitation, in Stable Isotope Geochemistry: A Tribute to Samuel Epstein, edited by H.P. Taylor, et al., *Spec. Publ. R. Soc. Chem., 3*, 169-185, 1991.

Morinaga, H., C. Itota, N. Isezaki, H. Goto, K. Yaskawa, M. Kusakabe, J. Liu, Z. Gu, B. Yuan, and S. Cong, Oxygen-18 and carbon-13 records for the last 14,000 years from lacustrine carbonates of Siling-Co lake in the Qinghai-Tibetan Plateau, *Geophys. Res. Lett., 20*, 2909-2912, 1993.

Merlivat, M., and J. Jouzel, Global climatic interpretation of the deuterium - oxygen-18 relationship for precipitation, *J. Geophys. Res., 84*, 5029-5033, 1979.

Perry, A. H. and J. M. Walker, *The Ocean-Atmosphere System*, Longman, White Plains, N.Y., 1977.

Petit, J. R., J. W. C. White, N. W. Young, J. Jouzel, and Y. S. Korotkevich, Deuterium excess in recent Antarctic snow, *J. Geophys. Res., 96*, 5113-5122, 1991.

Ren, M., *An Outline of China's Physical Geography, China Knowledge Ser.*, Foreign Languages Press, Beijing, 1985.

Rozanski, K., and L. Araguás-Araguás, Spatial and temporal variability of stable isotope composition of precipitation over the South American continent, Bull. Inst. Fr. d'Etud. Andines, *24(3)*, 379-390, La Paz, 1995.

Rozanski, K., C. Sonntag, and K. O. Munnich, Factors controlling stable isotope composition of modern European precipitation, *Tellus, 34*, 142-150, 1982.

Rozanski, K., L. Araguás-Araguás, and R. Gonfiantini, Isotopic patterns in modern global precipitation, in *Climate Change in Continental Isotopic Records, Geophys. Monogr. Ser*, vol. 78. edited by P.R. Swart, et al., pp. 1-36, AGU, Washington D.C., 1993.

Rozanski, K., L. Araguás-Araguás, and R. Gonfiantini, Isotope patterns of precipitation in the East African region, in *The Limnology, Climatology and Paleoclimatology of the East African Lakes*, edited by T.C Johnson and E.O. Odada, pp. 79-93, Gordon and Breach., Newark, N. J., 1996.

Salati, E., A. Dall'Olio, E. Matsui, and J. R. Gat, Recycling of water in the Amazon Basin: An isotopic study, *Water Resour. Res., 15*, 1250-1258, 1979.

Siegenthaler, U., and H. Matter, Dependence of ^{18}O D in precipitation on climate, in *Paleoclimate and Paleowaters: A Collection of Environmental Isotope Studies*, pp. 37-51, Int. At. Energy Agency, Vienna, 1983.

Sonntag, C., K. Rozanski, K. O. Münnich, and H. Jacob, Variations of deuterium and oxygen-18 in continental precipitation and groundwater and their causes, in *Variations in the Global Water Budget*, edited by A. Street-Perrott et al., pp. 107-124, D. Reidel , Norwell, Mass., 1983.

Thompson, L. G., E. Mosley-Thompson, M. E. Davis, J. F. Bolzan, J. Dai, T. Yao, N. Gundestrup, X. Wu, L., Klein, and Z. Xie, Holocene-Late Pleistocene climatic ice core records from Qinghai-Tibetan Plateau, *Science, 246*, 474-477, 1989.

Van der Straaten, C. M., and W. G. Mook, Stable isotope composition of precipitation and climatic variability, in *Paleoclimate and Paleowaters: A Collection of Environmental Isotope Studies,* pp. 53-64, Int. At. Energy Agency, Vienna, 1983.

Winkler, M. G., and P. K. Wang, The Late-Quaternary vegetation and climate of China, in *Global Climates Since the Last Glacial Maximum,* edited by H.E. Wright et al., pp. 221-261, Univ. of Minn. Press, St. Paul., 1993.

Yakir, D., and X. F. Wang, Fluxes of CO_2 and water between terrestrial vegetation and the atmosphere estimated from isotope measurements, *Nature, 380*, 515-517, 1996.

Yapp, C. J., A model for the relationships between precipitation D/H ratios and precipitation intensity, *J. Geophys. Res., 87*, 9614-9620, 1982.

Yurtsever, Y., and J. R. Gat, Atmospheric waters, in Stable Isotope Hydrology: Deuterium and Oxygen-18 in the Water Cycle, edited by J. R. Gat and R. Gonfiantini, *Tech. Rep. Ser.* vol. 210, pp. 103-142, Int. At. Energy Agency, Vienna, 1981.

L. Araguás-Araguás and K. Froehlich; Isotope Hydrology Section, International Atomic Energy Agency, Wagramer Strasse 5, P.O. Box 100, Vienna A-1400, Austria. (K.Froehlich@iaca.org)

K. Rozanski, Faculty of Physics and Nuclear Techniques, University of Mining and Metallurgy, 30-054 Krakow, Poland. (rozanski@novell.ftj.agh.edu.pl)

(Received December 31, 1997; revised July 16, 1998;
accepted July 20, 1998.)